

A model for the study of *Helicobacter pylori* interaction with human gastric acid secretion

Ian M. Joseph, Denise Kirschner*

Department of Microbiology and Immunology, The University of Michigan Medical School, 6730 Medical Science Building II,
Ann Arbor, MI 48109-0620, USA

Received 12 September 2003; received in revised form 5 December 2003; accepted 8 December 2003

Abstract

We present a comprehensive mathematical model describing *Helicobacter pylori* interaction with the human gastric acid secretion system. We use the model to explore host and bacterial conditions that allow persistent infection to develop and be maintained. Our results show that upon colonization, there is a transient period (day 1–20 post-infection) prior to the establishment of persistence. During this period, changes to host gastric physiology occur including elevations in positive effectors of acid secretion (such as gastrin and histamine). This is promoted by reduced somatostatin levels, an inhibitor of acid release. We suggest that these changes comprise compensatory mechanisms aimed at restoring acid to pre-infection levels. We also show that ammonia produced by bacteria sufficiently buffers acid promoting bacteria survival and growth.

© 2003 Elsevier Ltd. All rights reserved.

Keywords: *Helicobacter pylori*; Gastric acid; Persistence; Mathematical model

1. Introduction

Helicobacter pylori causes inflammation of the gastric mucosa (gastritis) that may predispose infected individuals to develop ulcers or gastric tumors (Kitahara et al., 1998). Most colonized individuals (~80%) remain asymptomatic, presenting with mild but diffuse inflammation of the stomach and show little or no atrophy throughout their lifetimes (Kapadia, 2003; Moayyedi et al., 2000; Prinz et al., 2003). A small percentage (0.1–4%) of chronically infected individuals, however, develop severe disease (gastritis) involving both corpus and antrum regions of the stomach. This leads to a diminished acid secretory capacity (Kapadia, 2003; Uemura et al., 2001). Disease may eventually progress to adenocarcinoma requiring treatment (Prinz et al., 2003; Uemura et al., 2001). Upon infection, three clinical outcomes are possible: (1) bacterial eradication or clearance, usually after treatment (Takimoto et al., 1997; Ulmer et al., 2003), (2) chronic or persistent, low-level, asymptomatic gastritis (Prinz et al., 2003; Uemura

et al., 2001) during which bacterial population sizes remain unchanged or in steady state, or (3) progression to severe disease such as atrophy of gastric glands, gastric ulcers or carcinomas (Kitahara et al., 1998; Prinz et al., 2003; Uemura et al., 2001). Given the spectrum of diseases associated with *H. pylori* infection, many studies focus on characterizing host and bacterial factors that contribute to disease progression (D'Elis et al., 1997a, b; El-Omar et al., 2000; Ibraghimov and Pappo, 2000; Josenhans and Suerbaum, 2002; Mahalanabis et al., 1996; Prinz et al., 2003; Rad et al., 2003).

H. pylori is a strict human pathogen (Cave et al., 1998), and therefore understanding the pathophysiology of *H. pylori*-associated diseases remains limited by constraints of patient studies (Graham, 2000) and animal models that do not faithfully explore the human disease. For example, the progression from initial colonization to disease development is complicated by the inaccessibility of the human stomach to repeated experiments. The limitation is also compounded by the lack of knowledge of timing of infection. A few studies with individuals who voluntarily ingest *H. pylori* or inadvertently become infected demonstrate that after inoculation with *H. pylori* early symptoms vary ranging from asymptomatic to clinical manifestations (Cave

*Corresponding author. Tel.: +1-734-647-7722; fax: +1-734-647-7723.

E-mail address: kirschne@umich.edu (D. Kirschner).

et al., 1998; McGowan et al., 1996). At the beginning of infection, patients with clinical manifestations present with nausea accompanied by stomach pain and halitosis due to ammonia production (induced by the bacterial enzyme urease—Cave et al., 1998; Morris and Nicholson, 1987). Gastritis of the whole stomach (pangastritis) usually ensues a week after ingestion followed by heavy colonization with bacteria (Cave et al., 1998).

Several studies also report profound but transient reductions in acid levels (hypochlorhydria) (Cave et al., 1998; Graham et al., 1988; Ramsey et al., 1979). Although hypochlorhydria coincides with increased inflammatory infiltrate and colonization of the corpus region of the stomach by *H. pylori* (Morris and Nicholson, 1987), the mechanisms responsible for hypochlorhydria in vivo still remain elusive. The involvement of the host immune response cannot be ruled out since several immune effectors such as interleukin-1 β (IL-1 β) potently suppress acid secretion from parietal cells (McGowan et al., 1996). IL-1 β is expressed in the gastric mucosa of infected individuals (Hwang et al., 2002) and is 100-fold more potent in inhibiting acid secretion than proton pump inhibitors (PPIs) prescribed to treat *H. pylori* (Wolfe and Nompleggi, 1992). Ammonia production by bacteria may also account for reduced acid secretion. All *H. pylori* strains shown to suppress acid levels in vivo are urease-positive suggesting that ammonia production may be important early in infection (Cave et al., 1998). Other unidentified bacterial effectors may also function as acid suppressors. In many infected individuals, several months after infection (2–9 months) acid levels return to normal by mechanisms that are not well understood (Ramsey et al., 1979). Resumption of normal acid levels may suggest down-regulation of bacterial effectors or the action of host compensatory mechanisms such as elevated gastrin levels (hypergastrinemia). If disease does not occur, a chronic infection develops usually with no further clinical detriment to the host.

There are no ideal animal models that completely mimic all diseases in humans attributed to *H. pylori* infection (Lee, 1998). This likely follows since human disease associated with *H. pylori* infection results from contributions from both microbe and human factors (Eaton, 1999). Therefore, although several animal models exist for studying various aspects of *H. pylori*-associated disease, underlying pathologies and asymptomatic disease state may differ from human disease (Lee, 1999). For example, characteristics of the inflammatory response differ in gnotobiotic piglets. After infection, infected piglets generally exhibit lower neutrophil infiltration of the gastric mucosa compared to adult humans (Lee, 1998; Nedrud, 1999). Mice, which are useful in understanding *H. pylori* pathogenesis, generally present with less inflammation (Nedrud, 1999).

While research into *H. pylori* pathogenesis has benefited from studying animal models, an integrated research approach is needed to understand the complexities associated with colonization of humans. Mathematical modeling, which offers such an approach, allows analyses of intricacies of host–microbe interactions, improving our understanding of persistence and disease progression. Persistence requires a delicate balance between the interaction of host and bacterial factors and may imply the existence of feedback mechanisms that are not currently characterized (Blaser and Kirschner, 1999; Kirschner and Blaser, 1995). It is possible that during *H. pylori*-associated diseases these feedback mechanisms are compromised. The existence of feedback mechanisms, key factors controlling system dynamics, and events leading to disease can be identified with the aid of mathematical models.

Previously we have proposed deterministic models describing *H. pylori* colonization dynamics (Blaser and Kirschner, 1999; Kirschner and Blaser, 1995). These models explore dynamics from acquisition of bacteria through development of host and bacterial populations in equilibrium; indicative of a persistent or chronic infection. The first model included feedback mechanisms in which bacteria, through monitoring host-derived nutrients, controlled induced inflammatory responses and bacterial population sizes (Kirschner and Blaser, 1995). These feedback mechanisms limit damage to the host and were important for maintenance of bacterial persistence. Furthermore, they demonstrated the importance of adherent bacteria in replenishing motile bacterial populations that are lost due to mucus shedding. The second model incorporated development of a non-specific host response concurrent with *H. pylori* persistence (Blaser and Kirschner, 1999). In this model, initial events following inoculation with *H. pylori* that lead to colonization were examined. Analysis of this model showed that the capacity of the host to respond accordingly to *H. pylori* determines the level of colonization. There is a lower bound on the host response capacity below which bacteria flourish, and an upper limit above which bacteria are cleared. These results again strengthen the hypothesis that bacterial–host co-regulatory mechanisms may be key for persistence. Although both models provide insight into *H. pylori* colonization, they do not assess the effect of host gastric physiology on bacterial colonization.

In this report, we present a model that builds on these previous mathematical models of *H. pylori* colonization dynamics by merging these ideas into our existing model of human gastric acid secretion (Joseph et al., 2003). Our human acid secretion model comprehensively describes regulation of acid release by key gastric effectors (Joseph et al., 2003). Specifically, we explored the effects of positive regulatory networks characterized by gastrin and histamine and a negative feedback

mechanism comprised of somatostatin on acid secretion. In our model, food served as the driving force stimulating a cascade of events that leads to acid release.

Our goal here is to develop a comprehensive model of *H. pylori*–host interactions that we will use in future studies to explore the effects of host and bacterial factors in determining colonization dynamics. As mentioned earlier, three outcomes are possible (i.e. clearance, persistence, or disease); however, we focus our study only on persistence, and demonstrate that under baseline conditions of normal acid secretion, persistence is achieved. Furthermore, we demonstrate the presence of compensatory mechanisms aimed at restoring normal acid levels. We also show that ammonia and bicarbonate produced by bacteria during urea hydrolysis sufficiently buffer acid thus creating a suitable environment for bacterial survival and growth.

2. The model

Previously we described a two-compartment model of human gastric acid secretion that now serves as the context for our *H. pylori* studies (Joseph et al., 2003). In that model, we defined two histologically distinct regions of the stomach, the antrum and corpus. The relevant regulatory elements responsible for maintenance of acid homeostasis occur in these compartments and include cell populations, secreted effectors, neurotransmitters, bicarbonate, and acid (Joseph et al., 2003). By virtue of the nature and function of the mucus lining, there exists a chemical (i.e. pH and bicarbonate) gradient across the mucus barrier (Engel et al., 1984; Schreiber et al., 2000). This suggests that bacteria near the lumen experience a different chemical environment to those near the gastric epithelia. For example, while antral bacteria near the epithelia experience a relatively constant pH of 7, those at the lumen are subjected to fluctuations ranging from pH 2–5 (see Fig. 1; Chen et al., 1997). We hypothesize that chemical gradients also exist for nutrients, urea, and ammonia present in mucus. To incorporate different chemical gradients encountered by *H. pylori*, we update our previous model to reflect spatial aspects of gastric physiology by including both luminal and epithelial regions (see Fig. 1). Additionally, we track bacteria in each region in the antrum and corpus. The components of the *H. pylori*–host model and assumptions are indicated below. In addition, the mathematical details are included in Appendix A.

We build a comprehensive model of *H. pylori* and its interactions with the gastric acid secretion system by tracking bacterial populations and factors they produce such as ammonia used in buffering acid (Sidebotham et al., 2003) and Cag and VacA proteins involved in enhancing host cell apoptosis (Jones et al., 1999; Megraud, 2001; Suzuki et al., 2002). We incorporated

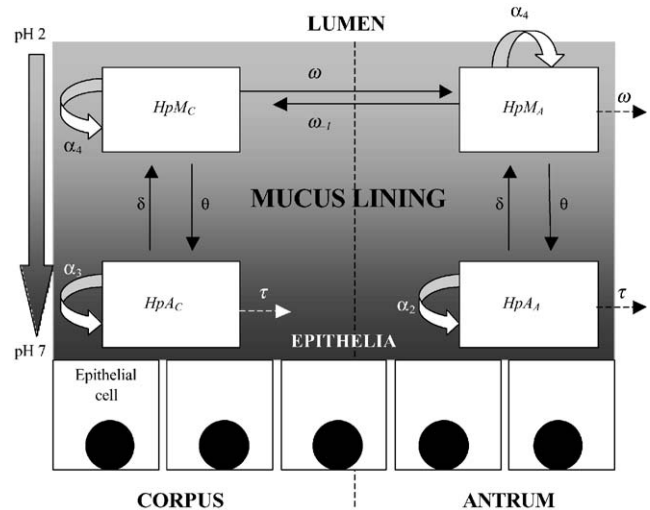


Fig. 1. Model diagram of *H. pylori* dynamics. Model includes dynamic changes in *H. pylori* populations in antrum and corpus. Each bacterial population encounters a different chemical environment. Bacteria near the lumen experience a pH of about 2 whereas those near epithelia are in a pH near 7. Both antrum and corpus compartments are subdivided into epithelial and luminal region to reflect these different pH levels. We include bacterial growth (α), loss (ω , ω_1 , and τ) and exchange (θ and δ) in each compartment: (1) motile (HpM_A) and (2) adherent (HpA_A) bacterial populations in the antrum and (3) motile (HpM_C) and (4) adherent (HpA_C) populations in the corpus. We assume that adherent bacteria are lost at a rate (τ) equivalent to epithelial cell sloughing while motile bacteria clear at rates equivalent to mucus shedding (ω). The vertical dashed line separates antral and corpus compartments.

these dynamics into our previously established gastric acid secretion model that included host factors such as gastrin, histamine, somatostatin, bicarbonate, and neural effectors, all of which are involved in acid regulation. To combine both models, we included relevant reactions at the biochemical level such as acid buffering by ammonia and bicarbonate ions produced during urease-catalysed urea hydrolysis (Fig. 2). We describe below why each of these factors is necessary and how they are incorporated into the model.

2.1. Bacterial components

2.1.1. *H. pylori*

We monitor *H. pylori* populations in both the antrum and corpus (Fig. 1). We simulate an inoculation of the corpus lumen with a specified *H. pylori* dose of 10^4 bacteria, the minimum infectious dose of *H. pylori* J166 in rhesus monkeys (Solnick et al., 2001). To simulate dynamical changes in *H. pylori* populations in the antrum and corpus we follow bacterial growth, loss and exchange of two different populations in each stomach region: (1) motile (HpM_A) and (2) adherent (HpA_A) bacterial populations in the antrum and (3) motile (HpM_C) and (4) adherent (HpA_C) populations in the corpus. Evidence for two bacterial subpopulations within each region (antrum and corpus) of an infected

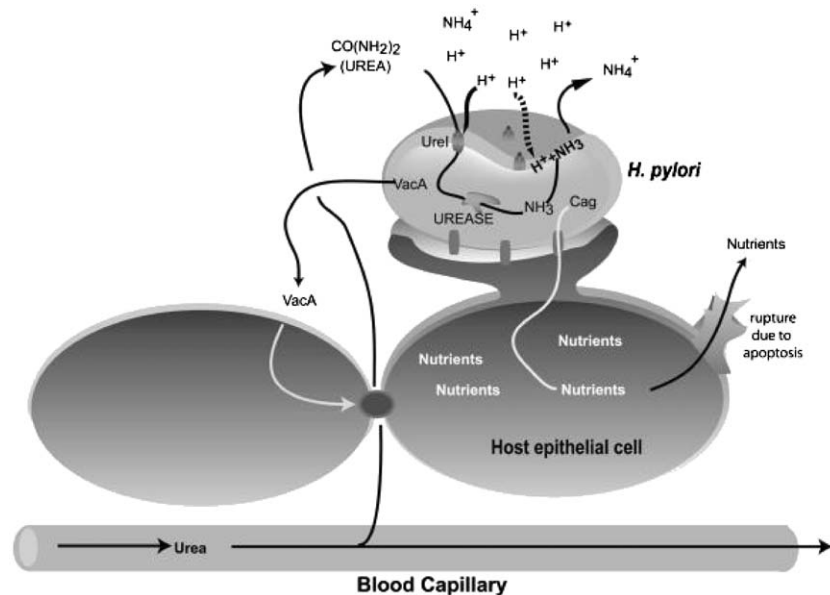


Fig. 2. Schematic diagram of the biochemical interactions. *H. pylori* adhering to an epithelial cell is shown. Bacteria passively uptake urea in an acid-dependent manner through UreI channels in bacterial membranes. Once in the cytoplasm urea is hydrolysed by urease enzymes to ammonia (NH_3) that diffuses across the periplasmic space to buffer acid. The by-product of buffering is the production of ammonium (NH_4^+) ions that diffuse into the mucus lining. We also show the effects of *VacA* in enhancing urea diffusion across tight junctions of gastric epithelial cells as well as its role together with *Cag* protein in inducing apoptosis.

host comes from several studies suggesting that free-swimming, flagellated bacteria (*HpM*) comprise the majority of bacteria in the stomach (~95%) (Hessey et al., 1990; Thomsen et al., 1990). A small proportion of bacteria (~5%; *HpA*) become aflagellated and attach to epithelial cells via adherence pedestals formed by host cell cytoskeletal rearrangements (Thomsen et al., 1990). Although the ratio of *HpM:HpA* is high, this may not be necessary for persistence of *H. pylori* within the host (Kirschner and Blaser, 1995). The dynamics of *H. pylori* populations are mathematically complex (see Appendix). Not only are differences in growth and loss characteristics of each population included, but we also track population site exchanges as well. One clinical outcome is studied in our current model: *persistence*; defined as bacterial population sizes in equilibrium or steady state.

While *H. pylori* colonize an acidic environment, it is a neutrophile growing over a limited pH range (~pH 6–8) with optimal growth at pH 7 (Fig. 3) (Sachs et al., 2000). Fig. 2 shows the result of simulating pH dependent growth of *H. pylori* (line) as compared with experimental results (bars). We include a pH-dependent growth term and compare our simulations with experimental results (Fig. 3).

Motile *H. pylori* near the epithelial boundary are able to attach to host epithelial cells provided adhesion sites exist. Research is ongoing to identify adhesins (such as Lewis antigens) expressed by bacteria that aid in adhesion (e.g., Webb and Blaser, 2002). The importance of adhesion for colonization and hence persistence is

evidenced by several experiments involving inhibition of bacterial adhesin binding to host phospholipid and glycosphingolipid receptors (Huesca et al., 1993; Kamisago et al., 1996). Previous mathematical models of *H. pylori* colonization also demonstrate that adherence is central to *H. pylori* colonization (Blaser and Kirschner, 1999; Falk et al., 2000; Kirschner and Blaser, 1995). When parameters governing the ability of bacteria to adhere were changed to create a 'virtual' mutant, the model predicted loss of colonization. These studies show that *H. pylori* colonies are significantly reduced or cleared during inhibition or deletion of adhesion unless bacteria alter components to compensate for the lack of adhesion.

Replenishment of the motile population is particularly important, as bacteria are lost due to natural processes of mucus shedding and epithelial sloughing (Kirschner and Blaser, 1995). We assume motile bacteria loss occurs at a constant rate due to mucus shedding. While adherent bacteria are lost during natural epithelial cell sloughing (Blaser and Kirschner, 1999; Kirschner, 1999), we assume this is enhanced by bacterial-mediated, host cell apoptosis (McGowan et al., 1996) (see discussion next paragraph). We speculate that bacteria migrate from antrum to corpus. We also allow for motile *H. pylori* in the antral region to flow back to the corpus region replenishing bacterial populations at that site. This becomes necessary because without antral to corpus bacterial exchange we do not observe corpus bacterial proliferation experimentally observed during suppression of acid secretion (Ohara et al., 2001; Tsutsui et al., 2000).

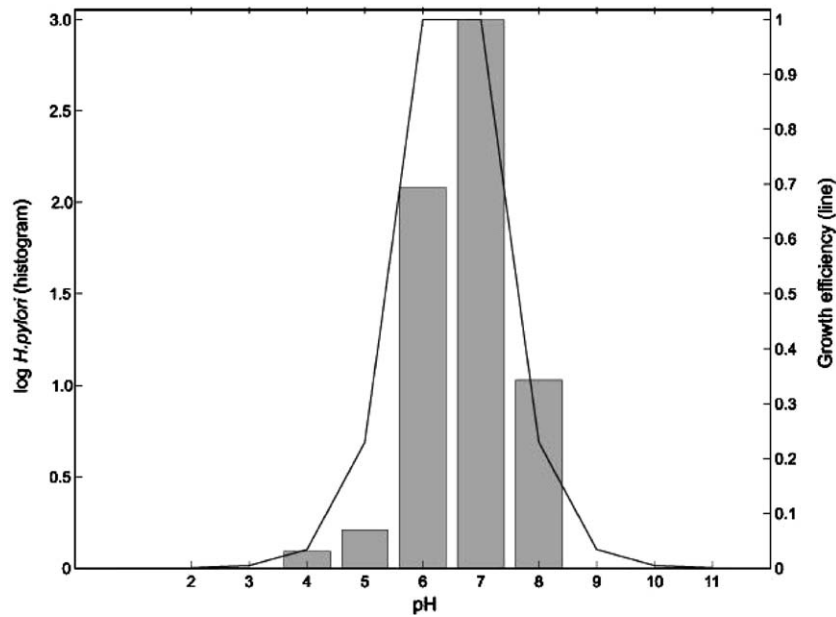


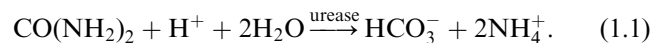
Fig. 3. pH-dependent growth of *H. pylori*. On the left axis (bar chart) *H. pylori* show optimal growth at pH 7 (Sachs et al., 2000). On the right axis we show our results of simulating pH-dependent growth (solid line) for use in the model.

Bacteria express Cag and VacA proteins that together with ammonia have been implicated in host cell death (Jones et al., 1999; Megraud, 2001; Suzuki et al., 2002). Upon insertion of Cag effectors into host cells via a type IV secretion apparatus, signal transduction cascades are initiated that lead to the upregulation of host cell apoptotic factors (Megraud, 2001) (Fig. 2). The role of VacA in apoptosis was recently demonstrated in a study involving the in vitro analysis of purified VacA on cultured gastric epithelial cells (Cover et al., 2003). Ammonia causes mucosal injury, reduces healing and induces apoptosis of gastric epithelial cells by releasing cytochrome c from mitochondria, an initial step of an apoptotic cascade (Suzuki et al., 2002). Taken together, bacterial loss, growth and site exchange adequately describe *H. pylori* changes over the time course of simulations. We now discuss in detail the role of each bacterial factor in pathogenesis.

2.1.2. Ammonia and ammonium production

Bacteria use ammonia produced during hydrolysis of urea by urease (Eq. (1.1)) to buffer external acid thereby creating a suitable pH niche (Sachs et al., 2000). Because *H. pylori* colonizes a highly acidic environment, it is not surprising that *H. pylori* has one of the highest urease activities of all known bacteria (Williams et al., 1996). Upon bacterial uptake of urea through acid-activated UreI channels, cytoplasmic urease enzymes hydrolyse urea to ammonia and bicarbonate ions (Sachs et al., 2000; Scott et al., 2000, 2002; Weeks et al., 2000; Weeks and Sachs, 2001). Uncharged ammonia then diffuses into the periplasmic space where it associates with protons to produce ammonium ions (Fig. 2; Sachs et al.,

2003). Ammonia produced can potentially alkalize external pH to a range that can support survival and growth of *H. pylori* (Sidebotham et al., 2003). Indeed, mutants for urease activity are unable to colonize gnotobiotic piglets indicating that urease expression, and subsequent ammonia production, is essential (Eaton et al., 1991; Karita et al., 1995; Tsuda et al., 1994a, b). Whether or not bacteria infecting humans produce sufficient quantities of ammonia to allow survival and growth has not been determined. We track ammonia levels by simulating production via acid-dependent mechanisms and loss through buffering acid and diffusion



We also assume that ammonium and excess ammonia are lost via natural processes including washout (when gastric contents move into the intestines) and when ions diffuse across the gastric mucosa into the underlying capillary network.

VacA. VacA, an 88-kDa secreted bacterial protein, is a major virulence and pathogenic factor linked to severe gastric tissue damage (Tombola et al., 2001). One key question we explore is the role of VacA in the initial stages of colonization. VacA plays a role in apoptosis in vitro and this activity may be important in vivo as well. Controversy exists regarding the significance of VacA toxin secreted by *H. pylori* during in vivo infections. Although gastric erosion is observed during oral administration of VacA producing strains or purified VacA (Marchetti et al., 1995; Pelicic et al., 1999), both *vacA* mutant and wild type *H. pylori*

similarly induce severe gastritis (Ogura et al., 2000). The role of VacA in eliciting cell vacuolation of membranous compartments at late stages of the endocytic pathway has long been demonstrated (de Bernard et al., 1998). Recently, the role of VacA in enhancing the movement of urea, small ions and nutrient across tight junctions between epithelial cells was revealed (Fig. 2; Papini et al., 1998; Pelicic et al., 1999; Tombola et al., 2001). It is possible that the importance of VacA to colonization varies over the time course of infection.

2.1.3. *CagPAI*

The 40-kb *cag* pathogenicity island (*cagPAI*) expresses a type IV secretion apparatus through which bacterial effectors are secreted directly into host epithelial cells. Among the 30 open reading frames on *cagPAI* is an immunodominant antigen, CagA, that is now used to ensure *cagPAI* presence in vivo and in vitro (Odenbreit et al., 2000). The function of each *cagPAI* transcript is not fully known, except for their collective role in affecting changes in host response. Genes within *cagPAI*, exclusive of the *cagA* gene, transcribe products that elicit expression of IL-8, a pro-inflammatory cytokine, that activates infiltrating neutrophils. These infiltrating neutrophils augment mucosal damage releasing cell contents into the gastric milieu (Nakazawa, 2002). We describe these proteins collectively as “Cag protein” and accordingly include their dynamics.

Some researchers suggest that bacteria acquire nutrients from degraded cells although there is no experimental evidence to support this hypothesis (Montecucco et al., 1999; Nakazawa, 2002). Studies correlating Cag protein levels to nutrient levels have not been performed; however, we hypothesize that increased inflammation due to Cag protein releases nutrients for bacterial consumption (Fig. 2). We also assume that release of nutrients from apoptosis likely saturates as bacteria modulate activity to limit damage to their host (Blaser and Kirschner, 1999). We discuss in more detail the relation of Cag protein to nutrient acquisition in Appendix A.

2.2. Host components

To analyse the effect of *H. pylori* on host gastric acid secretion, we couple nonlinear ordinary differential equations describing bacterial dynamics to our model of human acid secretion (Joseph et al., 2003). To this end, we modified our human gastric acid secretion model (Joseph et al., 2003) by updating acid equations to reflect acid buffering by ammonia and additional bicarbonate ions secreted by bacteria, and incorporating equations for nutrient and urea levels. More detailed descriptions of the equations are found in Appendix A and in our previous paper (Joseph et al., 2003), but below we briefly summarize our human acid

secretion model and how we include nutrient and urea levels.

2.2.1. Host gastric acid secretion model

In our previous model, we captured the salient features of acid regulation by including dynamics describing food volume, effector cell populations and key effectors (Joseph et al., 2003). Food both directly and indirectly elicits release of positive effectors of acid secretion from cells found in the antrum and corpus regions of the stomach (Hersey and Sachs, 1995). We included a dynamic feeding function based on a standard American diet of three meals per day (at 0600, 1200, 1800 h) (Joseph et al., 2003). By comparing various modality patterns of feeding functions, we show that long-term dynamics of effector, bicarbonate and acid responses are qualitatively similar to results obtained using the more dynamic feeding function such as that used in our previous work (Joseph et al., 2003). Furthermore, numerical analyses suggest that effector, bicarbonate, and acid responses resulting from a constant feeding function (i.e. $Fd(t) = 0.5$ L) are an average of simulation outcomes generated using our dynamic feeding function. This is only true if the trajectories of the numerical solutions of effector, bicarbonate and acid levels are attractors (i.e. either limit cycles or stable nodes). Given the similarity of simulation results and the ease of visualization in the long-term simulation, we present results using a constant feeding function here.

Whereas positive mechanisms reinforce acid secretion, negative mechanisms serve to return acid to basal levels after stimulation resulting in acid homeostasis. With the release of acid into the lumen, gastric pH decreases until a negative feedback effector, somatostatin, is secreted from D cells in the antrum (Shulkes and Read, 1991; Uvnas-Wallensten et al., 1980).

2.2.2. Modifications to original gastric acid secretion model

Nutrients. In our model of *H. pylori*–host interactions, we simulate host nutrient levels available for bacterial consumption. Given the hypothesis that *H. pylori* acquire nutrients from apoptotic cells, we assume that in a stomach devoid of *H. pylori* there are basal levels of apoptosis, and hence nutrients. With infection, nutrient levels are elevated by the activities of VacA and Cag proteins. For simplification, we assume that food consumed by the host does not provide simple nutrients such as amino acids and simple sugars for *H. pylori* acquisition as is suggested in Mendz and Hazell (1995) and Nagata et al. (2003).

Urea. We track host-derived urea that bacteria degrade. Catabolism of proteins produces carbon dioxide, ammonium and bicarbonate ions (see Eq. (1.1); Atkinson and Bourke, 1987). To dispose of

potentially toxic ammonium and bicarbonate ions, mammals have the urea cycle through which excess ammonia is converted to urea that is transported to kidneys for excretion (Atkinson and Camien, 1982; Cheema-Dhadli et al., 1987). Although the kidneys are efficient at excreting urea, a small proportion of plasma urea diffuses across the gastric mucosa into the lumen of the stomach where low levels (~3 mM) are maintained (Mokuolu et al., 1997). At low pH (<4) bacteria take up

urea through UreI channels for urease catalysis (Scott et al., 2000).

3. Parameter estimation

Since the basis of this model comes from previously published work (Joseph et al., 2003), we present details on estimating only new parameters here. Table 1

Table 1
List of parameter values used in our *H. pylori* model

Initial condition	Description	Initial values	Units	References
$HpM_A(0)$	Antral motile bacteria	0	Bacteria	§
$HpA_A(0)$	Antral adherent bacteria	0	Bacteria	§
$HpM_C(0)$	Corpus motile bacteria	1×10^4	Bacteria	(Solnick et al., 2001)
$HpA_C(0)$	Corpus adherent bacteria	0	Bacteria	§
$[NH_3(0)]_{AL}$	Antral luminal ammonia levels	0	M	§
$[NH_3(0)]_{AE}$	Antral epithelial ammonia levels	0	M	§
$[NH_3(0)]_{CL}$	Corpus luminal ammonia levels	0	M	§
$[NH_3(0)]_{CE}$	Corpus epithelial ammonia levels	0	M	§
$[NH_4(0)]_A$	Antral ammonium levels	0	M	§
$[NH_4(0)]_C$	Corpus ammonium levels	0	M	§
$[Vac(0)]_A$	Antral VacA levels	0	M	§
$[Vac(0)]_C$	Corpus VacA levels	0	M	§
$[Cag(0)]_A$	Antral Cag protein levels	0	M	§
$[Cag(0)]_C$	Corpus Cag protein levels	0	M	§
$[Ure(0)]_{AL}$	Antral luminal urea levels	20.2	μM	§
$[Ure(0)]_{AE}$	Antral epithelial urea levels	28.9	μM	§
$[Ure(0)]_{CL}$	Corpus luminal urea levels	32.9	μM	§
$[Ure(0)]_{CE}$	Corpus luminal urea levels	76.2	μM	§
$[Nut(0)]_{AL}$	Initial antral luminal nutrient levels	0.0089	pM	§
$[Nut(0)]_{AE}$	Antral epithelial nutrient levels	0.1	μM	§
$[Nut(0)]_{CL}$	Corpus luminal nutrient levels	0.004	pM	§
$[Nut(0)]_{CE}$	Corpus epithelial nutrient levels	54.14	nM	§
Parameters	Description	Values	Units	References
a	Max. <i>H. pylori</i> growth rate	0.060–0.832 (0.532)	/h	(Andersen et al., 1997) (Mendz and Hazell, 1995) (Rosberg et al., 1991)
y	Growth yield constant	1×10^{-15}	M/bacteria	§
kN	[nutrient] at which growth is 50% max.	50	pM	§
τ	Loss rate due to normal epithelial sloughing	0.0083–0.0139 (0.0036)	/h	(Hattori and Arizono, 1988)
θ	Motile to adherent exchange rate	0.95	/h	§
$K1$	Antral carrying capacity	1.2×10^7	Unitless	§
$K2$	Corpus carrying capacity	3.6×10^7	Unitless	§
δ	Adherent to motile exchange rate	0.0678	/h	§
rt	Bacterial-induced apoptotic rate	0.023833	/h	(Szabo and Tarnawski, 2000)
f_1	Cag protein scaling factor	1×10^9	Unitless	§
f_2	VacA scaling factor	1×10^5	Unitless	§
vf	VacA, Cag and ammonia levels at which apoptosis is 50% maximal	10	μM	§
ω_r	Bacterial loss rate due to mucus shedding	0.5–0.33 (0.010)	/h	(Hattori and Arizono, 1988)
ω_{-1}	Bacterial return rate to corpus from antrum	1×10^{-6}	/h	§
A_{bcrit}	Optimal pH for growth	7	Unitless	(Sachs et al., 2000)

Table 1 (continued)

Initial condition	Description	Initial values	Units	References
ψ_{max}	Maximal urea hydrolysis rate	1100 ± 200	MM/min/mg	(Dunn et al., 1990)
k_{ANh}	Michaelis constant for urea uptake	0.01	M	§
k_{UrNh}	Michaelis constant for urease	0.3–300	mM	(Dunn et al., 1990) (Scott et al., 1998)
σ	Reaction rate of bicarbonate and protons	71110	l/M h	§
$diff_{NH}$	Diffusion rate of ammonia	1×10^{-4}	/h	§
om	Clearance rate of ammonium ions	0.825	/h	§
ϵ	Maximal rate of VacA activation	2×10^{-20}	/h bacteria	§
A_{vcrit}	Optimal pH of VacA	3	Unitless	(Cover et al., 2003)
ρ_{VacA}	VacA protein degradation rate	0.8	/h	§
χ	Cag protein production rate	2×10^{-18}	M/bacteria.h	§
ρ_{cag}	Cag protein degradation rate	0.03	/h	§
β_{NH}	Clearance rate of ammonia	$0.01 \cdot \beta_A$	/h	§
ϕ_1	Antral source of urea	2.77 (3.6)	mM	(Mokuolu et al., 1997)
ϕ_2	Corpus source of urea	(5.6)	mM	(Mokuolu et al., 1997)
l_{max}	Maximal VacA-enhanced diffusion rate of urea	6.013	M/hr	(Tombola et al., 2001)
$diff_{Ur}$	Diffusion rate of urea	39	mM/h	§
β_{Ur}	Transport rate of urea	β_A	/h	§
κ_{Ur}	Clearance rate of urea	κ_A	/h	§

Values presented in parentheses are values used for simulations. § denotes mathematically estimated values. M—molar; h—hour.

summarizes new parameters included in our new model, whereas Table 2 (see Appendix A) shows a list of parameters that we previously estimated. We give the details of estimating each parameter in Appendix A.

We estimated rates of all the model processes from published, human-derived experimental data whenever possible. In the absence of human data, we use animal data to derive order of magnitude estimates. Units of measurement differ from one study to another, and we must standardize our estimates. When both animal and human data are lacking, we rely on C code based on Latin hypercube sampling method (LHS) for order of magnitude estimates (Iman et al., 1981a, b). LHS allows for simultaneous random, and evenly distributed sampling of each parameter within a defined range. A matrix with m columns corresponding to the number of varied parameters and n rows for the number of simulations is obtained; n simulations are generated that show uncertainty in model outcomes due to parameter variations.

Parameter values also have an intrinsic uncertainty. This uncertainty comes from variation in rates obtained from studies conducted on individuals and in in vitro experiments. For our uncertainty analyses, we run 20 simulations (18 degrees of freedom; 24 h) varying a given parameter by a factor of 1000. This is repeated for each parameter in the system individually. We investigate uncertainty in all parameters using LHS (Blower and Dowlatabadi, 1994).

4. Baseline simulations

Having defined the model and estimated parameters, we solved the system of ordinary differential equations (ODEs) using appropriate numerical methods to obtain temporal dynamics for each model variable. Numerical solutions were obtained for a 3-month time-frame using MatLab's ode15s solver for stiff systems (MathWorks, Natick, MA) and compatible C-code based on LHS and PRC developed in our laboratory. Lacking human data on infectious doses, we used the minimal infectious dose of *H. pylori* J166 in rhesus monkeys (Solnick et al., 2001). Thus, we began our simulations with an initial inoculum of 10^4 bacteria to the lumen of the corpus region and compare our simulation results with experimental data whenever possible. Earlier we defined different infection outcomes, namely clearance, disease and persistence; however, we focus primarily on the establishment of steady-state or persistent bacterial populations. Baseline simulations that progress toward steady state are representative of colonization of a healthy individual infected with wild-type *H. pylori* under normal conditions. Unless otherwise specified, we perform our experiments over a 3-month time period to capture host and bacterial changes during the early or acute stage of infection before the resumption of normal acid secretion. At the end of this stage of infection, we speculate that changes to host physiology result in a trifurcation leading to one of three different clinical outcomes. Understanding the conditions necessary for

persistence may give insight into disease course. Below, we describe in detail simulation results and comparisons of some these results with experimental data.

Testing the model is particularly important as it demonstrates credibility of results generated during novel simulations. We rigorously compare our results with experimental human data to test our model when possible. Specifically, we use similarities in trends between our simulation results and experimental data, such as significant and consistent order of magnitude reductions or elevations in effector levels. We use Student's *t*-test to determine significant differences between populations or effectors of interest.

5. Results

Our simulations are conducted under baseline conditions of normal acid levels described in our previous model (Joseph et al., 2003). While simulations described in this work primarily test our model, we also obtain information regarding Cag and VacA protein dynamics and function in vivo. These results are novel in that they lend insight into dynamics of these proteins in vivo, and are experiments not yet performed in the wetlab. We anticipated that nutrient levels would be highly correlated to Cag and VacA protein levels as well as ammonia concentration. However, this is not the case as complex

trends in nutrient dynamics evolve during simulations that are inexplicable by mere correlations.

5.1. Bacterial dynamics

In our first experiment we simulated *H. pylori* dynamics within the stomach under baseline conditions. Baseline simulations of bacterial colonization dynamics are shown in Fig. 4. With an initial inoculum to the lumen of the corpus region, this experiment shows that bacterial persistence in the corpus and antrum is achieved and maintained after a transient period of observable growth lasting approximately 20 days (Figs. 4A and B). Corpus motile bacteria initially adhere to corpus epithelia as well as migrate to the antral compartment. When antral bacterial populations attain suitable levels to maintain growth towards steady-state levels (at about 10 days post-infection) based on the logistic growth we imposed (Fig. 4A), corpus bacteria are replenished and rebound towards equilibrium (Fig. 4B). Although, to our knowledge there are no human data describing total numbers of motile and adherent bacteria in each compartment (antrum and corpus), we nevertheless draw informative conclusions from our results. Both corpus and antrum support bacterial growth; however, our results predict that a significant number of bacteria are confined to the antrum ($p < 0.01$), indicative of antral-predominant

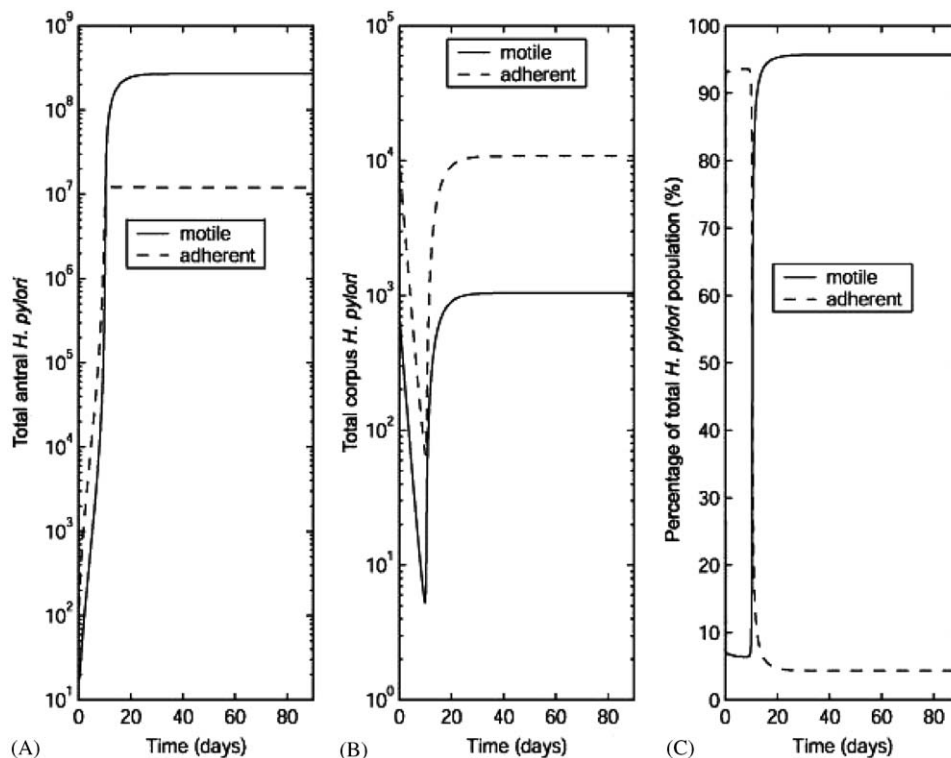


Fig. 4. Simulated changes in bacterial populations under baseline conditions. Adherent and motile bacterial population changes over time are shown in (A) the antrum and (B) corpus. (C) The total percent change of adherent and motile bacteria in both antrum and corpus.

gastritis in accordance with in vivo studies (Cave, 2001; Sanduleanu et al., 2001). In these studies conducted in patients with mild to moderate gastritis as defined by criteria described by Whitehead et al. (1972), approximately 99% of the bacteria were located in mucus and presumed to be motile. Our model predicts that total bacterial load (i.e. motile and adherent bacteria) supported by the antrum is on the order of 10^8 bacteria per total antrum and we assume that this may vary depending on the carrying capacity (i.e. size) of the antrum. Increasing the size of the antrum increases the number of adhesion sites available (Kirschner and Blaser, 1995); thus, bacterial load increases. Increasing bacterial load may have significant effects on gastric mucosa predisposing individuals to disease (Mullins and Steer, 1998). This is in drastic contrast to low bacterial populations supported in the corpus ($\sim 10^4$ bacteria per corpus). If we increase the size of the corpus capacity

however, the number of parietal cells correspondingly increases. This would likely increase acid levels creating an unsuitable environment for bacterial growth.

5.2. Host effector dynamics

We compared simulated dynamics of host dynamics with documented alterations to effectors in vivo. Our simulated host effector dynamics generally agree with known experimental data (Fig. 5). Immediately after infection, plasma gastrin levels significantly increase to a new steady state that is nearly two-fold greater than control levels (31.71 vs. 18.73 pM, respectively; $p < 0.01$; Fig. 5A), a trend consistent with experimental data (80 pg/ml for infected individuals vs. 47 pg/ml for uninfected controls) (Fig. 5B; Park et al., 1999; Park and Park, 1993). This rise in gastrin levels is primarily promoted by a similar two-fold decrease in total plasma

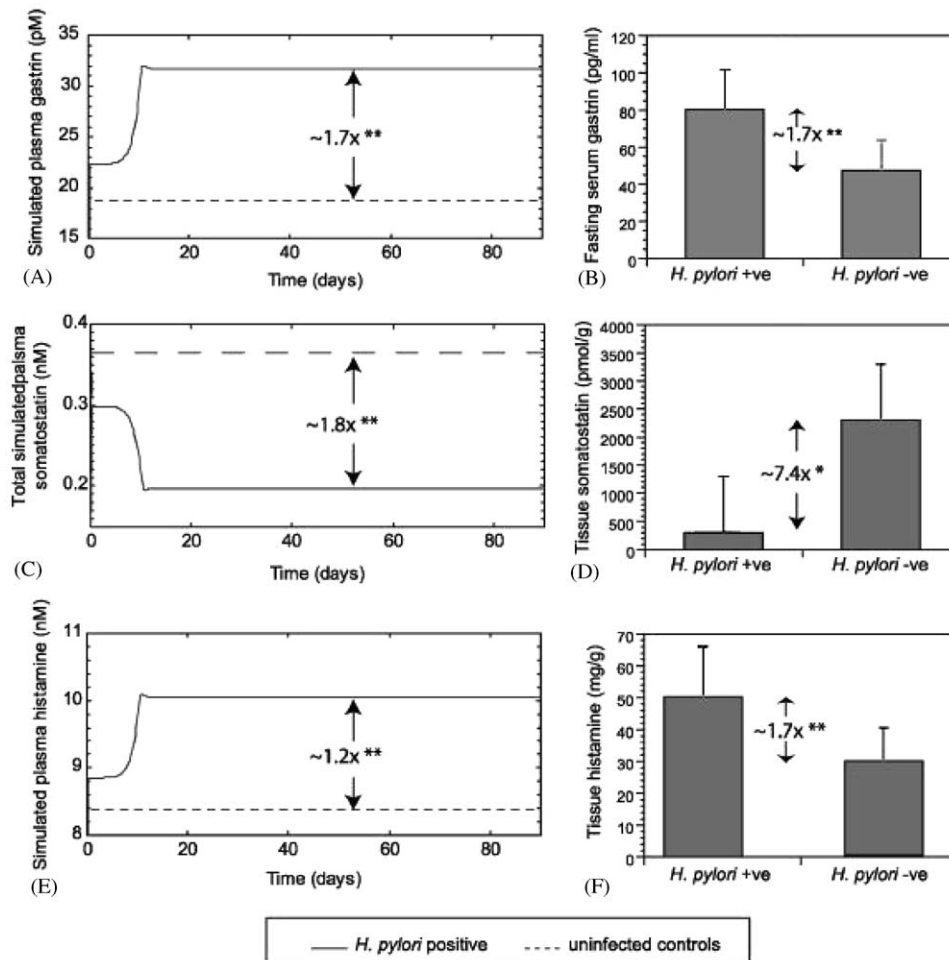


Fig. 5. Temporal changes in host effectors during infection with wild type *H. pylori*. Panels A, C and E show simulated plasma gastrin, somatostatin, and histamine, respectively. Panels B, D and F show experimental data on gastrin (Park et al., 1999; Park and Park, 1993), tissue somatostatin (Zavros et al., 2000), and histamine (Queiroz et al., 1991, 1993), respectively. The fold (x) change in effectors are shown for both simulated and experimental data. Single and double asterisks indicate significant differences of baseline results (solid line) at p -values of <0.05 and <0.001 , respectively, compared to uninfected controls (dashed line) as calculated by Student's t -test. The large fold difference between Panel C and D is discussed in the text.

somatostatin, an inhibitor of gastrin (0.20 nM during infection vs. 0.37 nM during healthy conditions; Fig. 5C). The differences between the role of antral and corpus somatostatin-secreting (D) cells is illustrated when we observe antral and corpus plasma somatostatin levels individually. The activities of antral bacteria increase antral pH, inhibiting pH-sensitive antral somatostatin secretion. Thus, we observe a significant decrease (~ 4.7 -fold) in antral somatostatin during *H. pylori* infection compared to controls (0.045 vs. 0.215 nM, respectively). In contrast, since corpus D cells are insensitive to changes in pH, somatostatin levels in this compartment remain relatively unchanged throughout the duration of the simulation (0.152 nM during infection vs. 0.150 nM during healthy conditions; data not shown). Similar trends are observed in experiments conducted in healthy and non-ulcer dyspepsia subjects where a seven-fold decrease in antral somatostatin was observed (310 pmol/g for *H. pylori*-infected individuals vs. 2318 pmol/g for uninfected individuals) with no change in corpus somatostatin content (220 pmol/g for *H. pylori*-infected persons vs. 148 pmol/g for control persons) (Zavros et al., 2000; Fig. 5D). In our model, changes in the antrum, such as higher gastrin levels, culminate in slightly increased histamine levels in the corpus (Fig. 5E). In vivo, a reduction in tissue histamine is observed (Fig. 5F; Queiroz et al., 1991, 1993). This decrease is due to reduced expression of histidine decarboxylase, the enzyme that catalyses production of histamine (Konturek et al., 2000); however, this enzyme and its effects are not included in our present model. Omission of histidine decarboxylase from our model appears to only affect histamine levels.

Deviations in effector levels are observed during the early stages of *H. pylori* colonization, but our simulations suggest that these changes are not a consequence of drastic alterations in cell population sizes that could potentially occur early in infection. Little is known experimentally about cell dynamics during the early stages of colonization (i.e. up to a month post-infection). However, our results suggest that during early-stage colonization, bacterial persistence is not a result of alterations in host cell populations (data not shown). For example, during simulations of early infection, G-cell populations in the stomach remain unchanged when compared to healthy controls (8.4×10^6 G cells in the total stomach for both positive and negative *H. pylori* controls; data not shown). This agrees with experimental results from studies in which they found that the number of G cells per gastric gland was not affected by infection (7.1 ± 3.1 in infected patients vs. 7.3 ± 3.9 in uninfected individuals) (Park et al., 1999). Similarly, we observe no significant changes in D, ECL and parietal cell populations (data not shown). This implies that abnormalities in acid regulation during early colonization are due to alterations in

the secretion of effectors rather than changes in proliferation or death of the cell populations themselves.

5.3. Ammonia effects on acid

A key question is whether or not bacteria produce sufficient ammonia in vivo to buffer acid. We find that ammonia produced by bacteria does sufficiently buffers host acid. In the absence of infection and during our simulated feeding conditions, corpus gastric pH decreases to a pH range between 2 and 3 due to acid secretion (data not shown). Similar pH decreases during feeding are observed in the antrum where pH ranges between 3 and 5, depending on region in the antrum (i.e., regions near the lumen or epithelial; Fig. 6A). The overall trend is an increase in gastric pH in infected individuals; however, the magnitude of increase in gastric pH varies between infected individuals and apparently depends on the type of ulceration that develops. In a study conducted by Furuta et al. the gastric pH of *H. pylori*-infected individuals diagnosed with various types of gastric ulcers (GU) was compared with control individuals (Furuta et al., 1998). The median gastric pH was 6.51 in proximal GU patients, 2.77 in distal GU patients, 1.71 in duodenal ulcer patients and 1.44 in control individuals (Furuta et al., 1998). Our simulations show that in the presence of *H. pylori* there is an almost 1.3-fold increase in antral pH near the epithelia during bacterial persistence (Fig. 6A). This falls within the range of similar changes observed by Annibale et al. (2003); Fig. 6B). We also note that although there is an increase in antral pH near the lumen, it is not significant. This result highlights the importance of the location within the mucus at which pH is sampled.

As resident bacterial populations proliferate (see Figs. 4A and B), ammonia levels also increase (Fig. 6C). Prior to achieving equilibrium, there is a peak in ammonia levels that we attribute to increases in corpus acid secretion during transiently declining corpus bacterial populations. Increased acid levels during this period require higher ammonia output by antral bacteria for sufficient buffering. Our simulation results show an increase in ammonia levels consistent with experimental data comparing ammonia levels in healthy and infected individuals (Fig. 6D; Furuta et al., 1998). We suggest that the observed reduction in acid levels is primarily due to buffering by bacterial ammonia and bicarbonate ions also produced during urea hydrolysis (Fig. 6C). Other supporting evidence includes both pH and ammonia achieving steady state levels at similar times (~ 10 days) post-infection (Figs. 6A and C). Although most bacteria are motile and non-adherent, these bacteria are limited by urea availability due to an established urea gradient. Prevailing ammonia levels near the lumen are considerably less than those near the

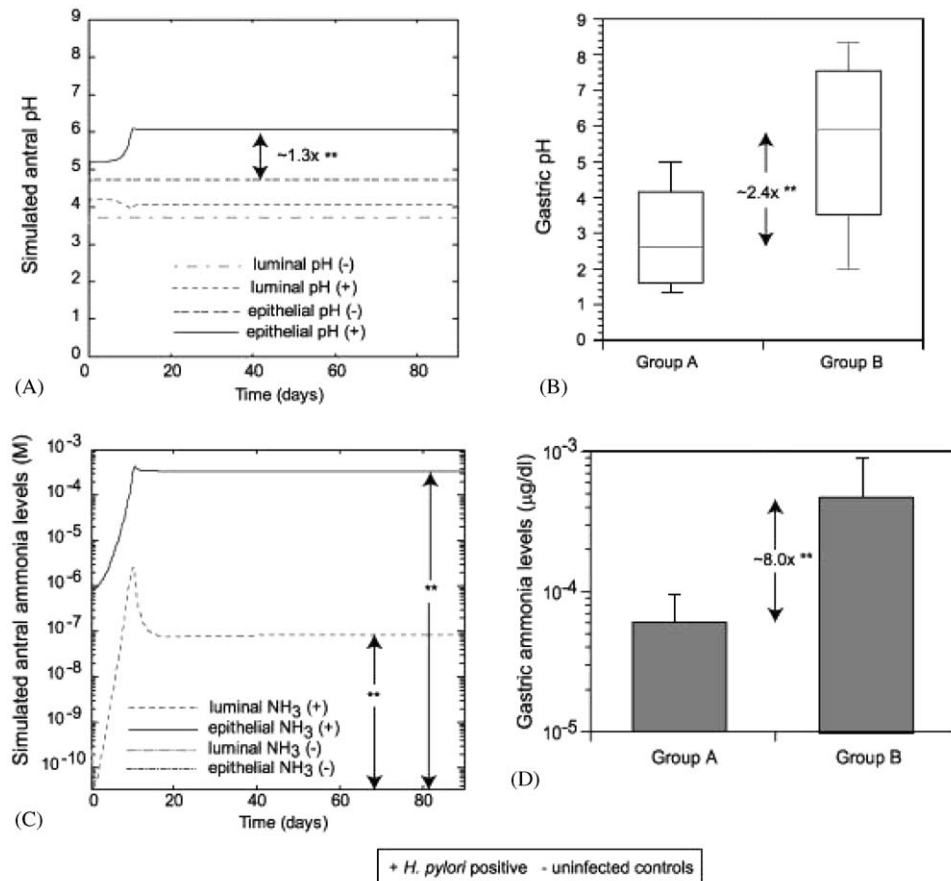


Fig. 6. Changes in acid levels corresponding to ammonia buffering. (A) Simulated antral acid levels over time during baseline and control conditions near the lumen and epithelia. (B) Experimental change in acid levels before (Group B) and after (Group A) infection with *H. pylori* from (Annibale et al., 2003). (C) Simulated dynamic changes in ammonia levels due to bacterial hydrolysis of urea. Simulated control values for luminal and epithelial ammonia levels are zero in the absence of *H. pylori* and therefore are not observable on a logarithmic scale. (D) Reported ammonia levels before (Group A) and after (Group B) infection with *H. pylori* (Furuta et al., 1998). The fold (x) change in pH and ammonia are shown for both simulated and experimental data. Single and double asterisks indicate significant differences of baseline results at p -values of <0.05 and <0.001 , respectively, compared to uninfected controls. Infected baseline results and uninfected controls are represented by (+) and (-), respectively.

epithelial surface ($p \leq 0.001$). To account for antral ammonia dynamics, ammonia influx from the corpus must also be considered. Whereas we show no ammonia production in the absence of *H. pylori*, low levels of ammonia can be measured experimentally (Fig. 6D) (Furuta et al., 1998) and are derived from host metabolism of amino acids not included in our model.

Modification of host acid levels due to *H. pylori* activity result in alterations of host effector levels. Increasing gastric pH due to ammonia buffering strongly inhibits somatostatin secretion and accounts for reduced antral somatostatin levels in our infected control scenario (see Fig. 5C). Lacking inhibition, gastrin levels increase significantly (see Fig. 5A). Our simulations suggest that ammonia levels produced by bacteria are sufficient to affect host acidity both directly and indirectly by altering host effector regulation, including the activity of compensatory mechanisms invoked to restore acid levels. The effects of host compensatory mechanisms are evident in our previous

work (Joseph et al., 2003) and are typically invoked to restore acid homeostasis during conditions of altered acid secretion.

5.4. Dynamics of bacterial effectors

We simulate both Cag and VacA proteins expressed by *H. pylori* to assess their activities on increasing nutrient availability in vivo. Cag proteins and VacA produced by *H. pylori* are expressed and may enhance nutrients or urea availability. Generally, levels of these proteins strongly correlate with bacterial numbers (see Figs. 7 and 4, respectively). As bacterial populations grow, Cag and VacA expression and secretion increase. Because both proteins may be long-lived (T. Cover, personal communication) and because VacA does not require bacterial adhesion to enter host cells, we simulate total activated VacA protein by pooling the amount expressed by both motile and adherent bacteria in their respective compartments. Note that subpicomolar

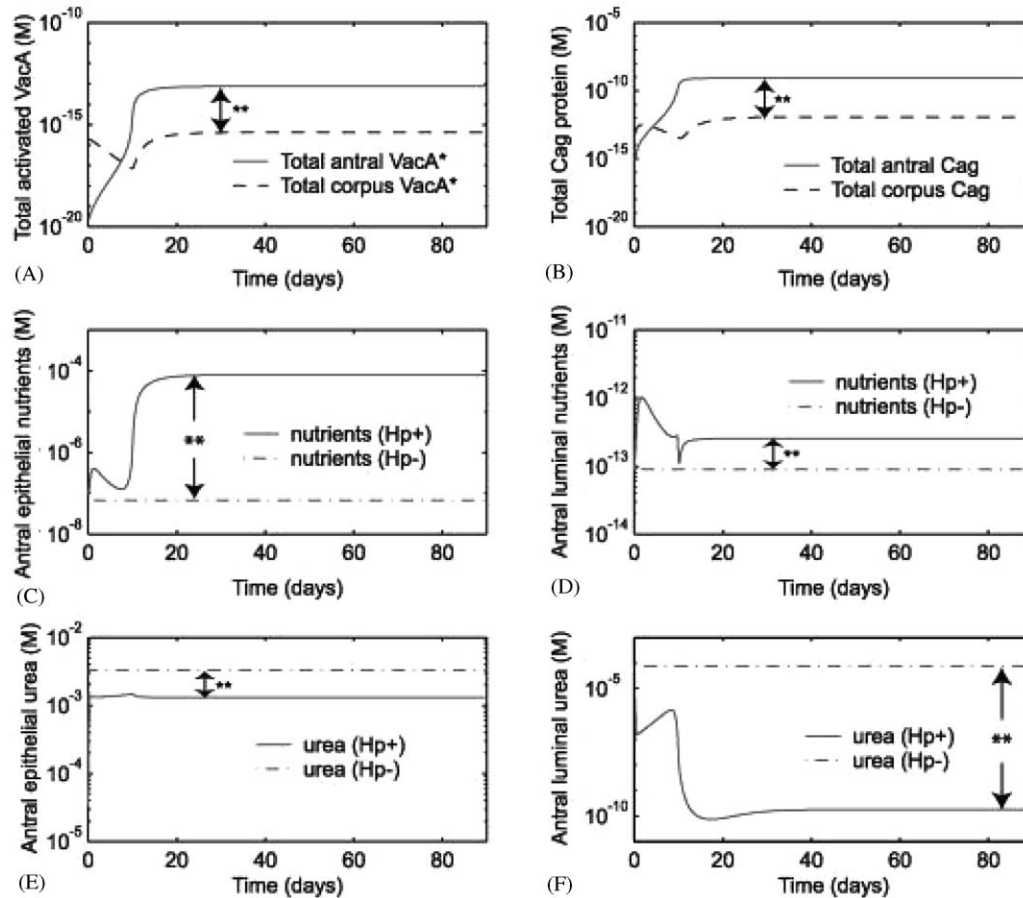


Fig. 7. The effects of Cag and VacA proteins on host nutrient and urea release. Panels A and B show dynamics of antral and corpus VacA and Cag protein levels, respectively. Panels C and D demonstrate fluctuations in antral nutrients at the epithelial and luminal surfaces, respectively. Panels E and F show changes in urea near the epithelia and luminal surfaces in the antrum and corpus, respectively. Double asterisks indicate significant differences of baseline results at p -values of <0.001 compared to uninfected controls. Hp+ indicates simulations with *H. pylori* present and Hp- suggests absence of *H. pylori*.

quantities of total VacA are expressed (Fig. 7A) in contrast to subnanomolar concentrations of Cag protein (Fig. 7B).

Because the majority of our simulated bacteria (99.9%) are located in the antrum, we focus on antral nutrients (Figs. 7C and D) and urea (Figs. 7E and F) levels enhanced by VacA and Cag protein action. Shortly post-infection (~ 10 days), simulated nutrient availability in the antrum rapidly increases above control levels (Fig. 7C). Prior to this point, sufficient infection has not been established in the antrum (Fig. 4A) to invoke noticeable nutrient release above basal levels (Fig. 7D) implying that an increase in nutrients is due to bacterial action. In the corpus approximately 10^3 bacteria (i.e. $\sim 10\%$ of the inocula) adhere to epithelial cells. This suggests a low level of colonization in the corpus which is observed experimentally with 1–5% of bacteria adhering to epithelial cells (Hessey et al., 1990; Thomsen et al., 1990; Kirschner, 1995, p. 162). The remaining 10^4 bacteria ($\sim 90\%$) fail to adhere comprising the motile population in the corpus.

Cag and VacA proteins expressed by these bacteria together with VacA protein secreted by motile bacteria promote epithelial cell apoptosis, releasing nutrients. Immediately post-infection, antral nutrient levels rapidly increase due to nutrient outflux from the corpus, the site of inoculation. However, with the decrease in corpus bacteria immediately after infection, VacA and Cag proteins also decrease resulting in the apparent, transient reduction in nutrient levels until day 10. In Fig 4B, the transient decrease in corpus bacteria and subsequent increase in antral population is due to migration of bacteria. As infection progresses, simulated nutrients levels attain a steady state level that is significantly elevated over control levels (Figs. 7C and D, $80.5 \mu\text{M}$ vs. 67.7 nM and 0.26 pM vs. 0.09 pM , respectively near the antral epithelia and lumen respectively, $p < 0.001$ for both). These nutrient levels are sufficient to support bacterial populations in the corpus and antrum. Bacterial products near the epithelia and lumen significantly decrease urea to levels below those of healthy controls ($p < 0.001$ for both; Figs. 7E and F).

Given that the ratio of motile bacteria to adherent bacteria is large, it is not surprising that antral motile bacteria hydrolyse more urea than adherent bacteria (Figs. 7E and F). In addition, antral motile bacteria experience lower pH levels thus requiring higher ammonia levels for buffering. In the antrum (Figs. 7E and F) and corpus (data not shown), a transient period occurs prior to day 10 during which urea levels appear to return to near pre-infection control levels. This is due to increased urea influx into the antrum from the corpus where bacterial populations initially decline thereby decreasing urea hydrolysis prior to day 10. However, after this transient period, urea near the epithelia and lumen attains steady state levels that are significantly lower than those in healthy controls (Figs. 7E and F, 13 vs. 33 mM and 0.18 nM vs. 76.1 μ M near the antral epithelia and lumen, respectively, $p < 0.001$ for both).

Our results described above of baseline and healthy controls adequately capture known host and bacterial dynamics. The simulated data of early stage infection are supported by experimental evidence and suggest that *H. pylori* affect changes in the host gastric system to allow for their colonization and persistence.

6. Discussion

We have developed a novel mathematical model of *H. pylori* interactions with its host describing bacterial and host effector dynamics from the start of infection to persistence. We accomplish this by incorporating *H. pylori* into our previous model of gastric acid secretion and its regulation by various gastric effectors (Joseph et al., 2003). Our primary goal for this article is to demonstrate model consistency with appropriate experimental data.

Our simulations show that although corpus and antrum are colonized (Fig. 4), the majority of bacteria are found in the antrum indicative of antral-predominant gastritis described in literature. Antral-predominant gastritis readily occurs no matter the site of inoculation. In simulations we inoculated the antral lumen with bacteria and allowed the system to evolve (data not shown). Although a greater bacterial load ($> 10^6$ bacteria) was required to establish colonization, bacteria mainly colonized the antrum. Two important findings come from these results. First, acid, and not host immunity, is the primary force responsible for the development of antral-predominant gastritis. At the site of acid secretion, pH often attains levels not conducive to bacterial growth. Corpus bacteria produce insufficient quantities of ammonia to allow *H. pylori* to flourish in the corpus. Second, the number of bacteria used to inoculate different sites within the stomach (i.e. antrum vs. corpus) may vary. While acid plays an important role in our second finding, we cannot exclude

the influence of washout of stomach contents in determining colonization. Studies of transit times of different meals in the stomach show that emptying of a liquid meal was more rapid than gastric emptying of a solid meal (Achour et al., 2001). We predict that as washout increases the likelihood of infection decreases (data not shown). Future experiments correlating the probability of infections with the type of contaminated foods consumed may yield additional insightful results regarding transmission of *H. pylori* infection.

We also demonstrated the effects of *H. pylori* activity on host effectors involved in regulation of acid homeostasis (Fig. 5). As bacteria alkalize the surrounding environment, our simulations show an inhibition of somatostatin release that promotes release of gastrin. These two gastric effectors together with histamine act in an antagonistic manner to regulate acid secretion. In our previous model of gastric acid secretion, we demonstrated that gastrin plays an important compensatory role in restoration of normal acid levels. In particular, we showed that gastrin levels, and not that of other gastric effectors, was altered consistently during various deletion scenarios.

In the presence of elevated gastrin levels during infection, an increase in acid levels is anticipated, but not observed. This is in part due to buffering of secreted acid by ammonia produced by corpus bacteria. However, in vivo activity of other host and bacterial factors not included in our model may augment inhibition of acid secretion. For example, the host pro-inflammatory cytokine, interleukin- 1β (IL- 1β), has been shown to potentially inhibit acid secretion from parietal cells (McGowan et al., 1996). These direct and indirect effects on acid secretion may represent adaptive mechanisms to allow colonization and persistence. We hypothesize that if these adaptive mechanisms function properly by allowing the establishment of colonization with little damage to the host, then persistence is achieved. Under certain circumstances, interactions of host and bacterial factors alter the system to such an extent that a new disease equilibrium is achieved. From experimental evidence, this disease state is not stable as clearance of bacteria through treatment can reverse *H. pylori* associated disease.

The role of VacA and Cag proteins cannot be ignored, as these proteins may be paramount to nutrient acquisition for *H. pylori*. However, these proteins appear not to be as important in events prior to persistence as their levels do not drastically alter outcome (Fig. 7). We speculate that these proteins assume greater importance by supporting higher bacterial levels during persistence. Recent discoveries of the role of VacA in enhancing urea diffusion across tight junction of the gastric epithelia have been included in our model (Tombola et al., 1999, 2001). However, no effect of VacA in this role was observed. Further study

would be required to elaborate this observation. Indeed, given the absence of evidence to suggest otherwise, it may be possible that bacteria may regulate expression of these proteins. Density-dependence may be an important factor in the regulation of these proteins in vivo.

We present a tested model that may be used as a basis of future studies into the development of persistence as well as clearance and disease. A key question is what role does acid play in the other states (clearance and disease) not addressed in this work. Bacteria devote many resources (e.g. urease) to overcome the acid barrier to colonization and this model may provide insight into the contribution of each resource. Another key question is what role the host immune response plays in the progression to disease. Our research demonstrates that an immune response is not necessary for the development of persistence. From our preliminary uncertainty and sensitivity analyses, we suggest that the early transient period is the time during which distinctions between different infection outcomes occur. This time frame is too short for an adaptive immune response, but may suggest a role for innate immunity. Therefore, dynamics occurring during this period may be critical in determining infection outcome. Future studies will explore these and other questions.

Acknowledgements

This work is supported by the National Institute of Health Grant 1RO1 HL62119 and the University of Michigan Rackham Merit Fellowship. We thank Drs. Linda Samuelson, Juanita Merchant, Michael Savageau, Cary Engleberg and David Gammack for helpful comments. We would like to especially thank Dr. Victor DiRita for his critical review of this paper. We are also grateful to Dr. Jose Segovia-Juarez for developing C code for the analysis of uncertainty and sensitivity. Gastric biopsies were supplied by Drs. Nguyen Thuy Vinh, Nguyen N Thanh and Han van Mao (Center for Cancer Research, Hanoi, Vietnam).

Appendix A

A.1. Bacteria and bacterial factor dynamics

Bacterial equations: We present a two-compartmental model comprising two histologically distinct stomach regions: antrum (subscript *A*) and corpus (subscript *C*). We further subdivide each compartment into the luminal (subscript *L*) and epithelial (subscript *E*) boundaries to describe events occurring in each region of the antrum and corpus. In each compartment we describe two bacterial phenotypes. Adherent bacteria (*H_{pA}*) are confined to the epithelial boundary and

contribute to events occurring there whereas motile bacteria (*H_{pM}*) are found near the luminal boundary. We begin with the description of the rates of changes of *H_{pA}* and *H_{pM}* populations in the antrum and corpus compartments (Eqs. (A.1)–(A.4)).

$$\begin{aligned} \frac{dH_{pA_A}(t)}{dt} = & \alpha_2([pH_{A_{AE}}(t)]) \cdot H_{pA_A}(t) \left(\frac{[Nut(t)]_{AE}}{[Nut(t)]_{AE} + k_N} \right) \\ & - \tau \cdot H_{pA_A}(t) + \vartheta \cdot H_{pM_A}(t) \\ & \times (1 - H_{pA_A}(t)/K_1) - \delta \cdot H_{pA_A}(t) - rt \\ & \times \frac{f_1[Cg(t)]_A + f_2[Vc(t)]_A + [NH_3(t)]_{AE}}{f_1[Cg(t)]_A + f_2[Vc(t)]_A + [NH_3(t)]_{AE} + vf} \\ & \times H_{pA_A}(t), \end{aligned} \quad (A.1)$$

$$\begin{aligned} \frac{dH_{pM_A}(t)}{dt} = & \alpha_1([pH_{A_{AL}}(t)]) \cdot H_{pM_A}(t) \left(\frac{[Nut(t)]_{AL}}{[Nut(t)]_{AL} + k_N} \right) \\ & - \varpi_1 \cdot H_{pM_A}(t) - \vartheta \cdot H_{pM_A}(t) \\ & \times (1 - H_{pA_A}(t)/K_1) + \delta \cdot H_{pA_A}(t) \\ & - \varpi_{-1} \cdot H_{pM_A}(t) + \varpi \cdot H_{pM_C}(t), \end{aligned} \quad (A.2)$$

$$\begin{aligned} \frac{dH_{pA_C}(t)}{dt} = & \alpha_3([pH_{A_{CE}}(t)]) \cdot H_{pA_C}(t) \left(\frac{[Nut(t)]_{CE}}{[Nut(t)]_{CE} + k_N} \right) \\ & - \tau \cdot H_{pA_C}(t) + \vartheta \cdot H_{pM_C}(t) \\ & \times (1 - H_{pA_C}(t)/K_2) - \delta \cdot H_{pA_C}(t) - rt \\ & \times \frac{f_1[Cg(t)]_C + f_2[Vc(t)]_A + [NH_3(t)]_{CE}}{f_1[Cg(t)]_C + f_2[Vc(t)]_A + [NH_3(t)]_{CE} + vf} \\ & \times H_{pA_C}(t), \end{aligned} \quad (A.3)$$

$$\begin{aligned} \frac{dH_{pM_C}(t)}{dt} = & \alpha_4([pH_{A_{CL}}(t)]) \cdot H_{pM_C}(t) \left(\frac{[Nut(t)]_{CL}}{[Nut(t)]_{CL} + k_N} \right) \\ & - \varpi \cdot H_{pA_C}(t) - \vartheta \cdot H_{pM_C}(t) \\ & \times (1 - H_{pA_C}(t)/K_2) + \delta \cdot H_{pA_C}(t) \\ & + \varpi_{-1} \cdot H_{pM_A}(t). \end{aligned} \quad (A.4)$$

Bacterial population changes are governed similarly by pH- and nutrient-dependent growth, loss, exchange and transfer between luminal and epithelial regions of the antrum and corpus. Appreciable *H. pylori* growth occurs over a narrow pH range (pH 6–8) with an optimal pH of 7 (see Fig. 2). We define a term that reproduces *H. pylori* growth characteristics, $\alpha \cdot ([pH_A(t)]) = a(1 - (\tanh([pH_A(t)] - A_{brit}))^2)$, depending on external pH. In this term *a* represents the maximal growth rate of *H. pylori*, *pH_A(t)* denotes the antral pH at a specific boundary, and *A_{brit}* is the optimal pH for growth. We include the following pH-dependent growth terms:

$$\begin{aligned} \alpha_1([pH_{A_{AL}}(t)]) \\ = a(1 - (\tanh([pH_{A_{AL}}(t)] - A_{brit}))^2), \end{aligned} \quad (A.5)$$

$$\begin{aligned} \alpha_2([pH_{A_{AE}}(t)]) \\ = a(1 - (\tanh([pH_{A_{AE}}(t)] - A_{brit}))^2), \end{aligned} \quad (A.6)$$

$$\begin{aligned} \alpha_3([pHA_{CE}(t)]) \\ = a(1 - (\tanh([pHA_{CL}(t)] - A_{bcrit}))^2), \end{aligned} \quad (\text{A.7})$$

$$\begin{aligned} \alpha_4([pHA_{CL}(t)]) \\ = a(1 - (\tanh([pHA_{CE}(t)] - A_{bcrit}))^2). \end{aligned} \quad (\text{A.8})$$

Growth is also dependent on nutrients that are limited in the stomach. To simulate nutrient-dependent growth we rely on the mathematically well-defined Monod kinetics, $Hp(t) \cdot ([Nut(t)]/([Nut(t)] + k_N))$. These kinetics are similar to Michaelis–Menten kinetics used to describe enzyme catalysis of a substrate. After an initial stage of exponential bacterial growth, nutrients become limiting reducing bacterial growth until an equilibrium is achieved.

As in (Blaser and Kirschner, 1999; Kirschner and Blaser, 1995), we include migration of bacteria between luminal and epithelial boundaries as well as bacterial loss. Motility and the spiral geometry of bacteria allow bacteria to burrow into the mucus lining that protects underlying stomach epithelial cells from the corrosive effects of acid (Ferrero and Lee, 1988). Once near the epithelia, bacteria encounter optimal pH conditions for growth. Also, bacteria near the epithelia are able to specifically adhere to stomach epithelial cells by inducing the formation of adhesion pedestals (Hessey et al., 1990). The acquisition of suitable adhesion sites limits the number of bacteria that are able to adhere to epithelial cells. Evidence in support of a “carrying capacity” comes from a morphometric study that determined that approximately 95% of *H. pylori* in the stomach were motile whereas only 5% adhered to epithelia (Thomsen et al., 1990). We define this exchange between adherent and motile bacteria using the term, $\vartheta \cdot HpM_A(t)(K_1 - HpA_A(t))$. Bacteria are lost from the stomach via mucus shedding and epithelia sloughing. We assume that these biological processes occur at a steady rate in the stomach and bacterial loss rates are proportional to these processes, (ω and ω_1 , respectively). A small percentage of bacteria are able to migrate from the antrum to the corpus against mucus flow and we include this ($\varpi_{-1} \cdot HpM_A(t)$). We also include increased adherent bacterial loss due to apoptosis invoked by cytotoxic Cag and VacA protein and ammonia. We describe this enhanced apoptosis as follows:

$$rt \frac{f_1[Cg(t)] + f_2[Vc(t)] + [NH_3(t)]}{f_1[Cg(t)] + f_2[Vc(t)] + [NH_3(t)] + vf} Hp(t), \quad (\text{A.9})$$

where f_1 and f_2 are scaling factors and rt the maximal bacterial loss rate due to apoptosis.

Ammonia and ammonium equations. To overcome the acid barrier to colonization, bacteria hydrolyse free urea to produce ammonia and bicarbonate ions (see Fig. 2 and Eq. (A.1)). We use the following differential equations (Eqs. (A.10)–(A.13)) to describe the rates of change of ammonia in each region (i.e. near the lumen

and epithelia) in the antrum and corpus:

$$\begin{aligned} \frac{d[NH_3(t)]_{AL}}{dt} \\ = \left(\psi_1([pHA_{AL}(t)]) \left(\frac{[Ur(t)]_{AL}}{[Ur(t)]_{AL} + k_{UrNh}} \right) HpM_A(t) \right) \\ - \sigma[NH_3(t)]_{AL}[A_{AL}(t)] - \kappa[NH_3(t)]_{AL} \\ + \beta[NH_3(t)]_{CL} - \text{diff}_{NH}[NH_3(t)]_{AL} \\ + p_1 \cdot \text{diff}_{NH}[NH_3(t)]_{CL}, \end{aligned} \quad (\text{A.10})$$

$$\begin{aligned} \frac{d[NH_3(t)]_{AE}}{dt} \\ = \left(\psi_2([pHA_{AE}(t)]) \left(\frac{[Ur(t)]_{AE}}{[Ur(t)]_{AE} + k_{UrNh}} \right) HpA_A(t) \right) \\ - \sigma[NH_3(t)]_{AE}[A_{AE}(t)] - \kappa[NH_3(t)]_{AE} \\ + \beta[NH_3(t)]_{CE} + \text{diff}_{NH}[NH_3(t)]_{CE} \\ + \text{diff}_{NH}[NH_3(t)]_{AL}, \end{aligned} \quad (\text{A.11})$$

$$\begin{aligned} \frac{d[NH_3(t)]_{CL}}{dt} \\ = \left(\psi_3([pHA_{CL}(t)]) \left(\frac{[Ur(t)]_{CL}}{[Ur(t)]_{CL} + k_{UrNh}} \right) HpM_C(t) \right) \\ - \sigma[NH_3(t)]_{CL}[A_{CL}(t)] \\ - \text{diff}_{NH}[NH_3(t)]_{CL} - \beta[NH_3(t)]_{CL}, \end{aligned} \quad (\text{A.12})$$

$$\begin{aligned} \frac{d[NH_3(t)]_{CE}}{dt} \\ = \left(\psi_4([pHA_{CE}(t)]) \left(\frac{[Ur(t)]_{CE}}{[Ur(t)]_{CE} + k_{UrNh}} \right) HpA_C(t) \right) \\ - \sigma[NH_3(t)]_{CE}[A_{CE}(t)] - \beta[NH_3(t)]_{CE} \\ + p_2 \cdot \text{diff}_{NH}[NH_3(t)]_{CL} - \text{diff}_{NH}[NH_3(t)]_{CE}, \end{aligned} \quad (\text{A.13})$$

$$\psi_1([pHA_{AL}(t)]) = \psi_{\max} \left(\frac{[pHA_{AL}(t)]}{[pHA_{AL}(t)] + k_{ANh}} \right), \quad (\text{A.14})$$

$$\psi_2([pHA_{AE}(t)]) = \psi_{\max} \left(\frac{[pHA_{AE}(t)]}{[pHA_{AE}(t)] + k_{ANh}} \right), \quad (\text{A.15})$$

$$\psi_3([pHA_{CL}(t)]) = \psi_{\max} \left(\frac{[pHA_{CL}(t)]}{[pHA_{CL}(t)] + k_{ANh}} \right), \quad (\text{A.16})$$

$$\psi_4([pHA_{CE}(t)]) = \psi_{\max} \left(\frac{[pHA_{CE}(t)]}{[pHA_{CE}(t)] + k_{ANh}} \right). \quad (\text{A.17})$$

Ammonia production is a complex, dynamic process optimized through regulatory mechanisms to efficiently buffer acid. In keeping with *H. pylori* physiology, we include pH-dependent urea hydrolysis terms (Eqs. (A.14)–(A.17)). Bacteria are shown to express a pH-sensitive, urea transport channel (UreI) that allows urea influx into the cytoplasm at low pHs (Mollenhauer-Rektorschek et al., 2002; Rektorschek et al., 2000; Weeks et al., 2000). At pH below 4, UreI channels in bacterial membranes adopt an open-conformation that permits the uptake of urea (Rektorschek et al., 2000). In

the cytoplasm, urea is hydrolysed by urease under Michaelis–Menten kinetics $[Ur(t)]/([Ur(t)] + k_{UrNh})$ to liberate ammonia and bicarbonate ions used for acid buffering. Together these mechanisms comprise the acid-adaptive strategies employed by *H. pylori* to evade acid. Ammonia and bicarbonate ions readily diffuse into the periplasmic space of the bacterial membrane where they react with protons (H^+) thus buffering acid. We assume that the milieu of the periplasmic space is well-mixed and therefore use a mass action term to describe this buffering reaction. This reaction yields ammonium ions that diffuse into the external environment (Eqs. (A.18) and (A.19)). We assume excess unreacted ammonia together with ammonium are released into the external environment where they are lost by diffusion and mucus transport to other regions of the stomach and intestines

$$\frac{d[NH_4]_A}{dt} = \sigma[NH_3(t)]_{AL}[A_{AL}(t)] + \sigma[NH_3(t)]_{AE}[A_{AE}(t)] - om[NH_4]_A, \quad (A.18)$$

$$\frac{d[NH_4]_C}{dt} = \sigma[NH_3(t)]_{CL}[A_{CL}(t)] + \sigma[NH_3(t)]_{CE}[A_{CE}(t)] - om[NH_4]_C. \quad (A.19)$$

VacA equations. The function of VacA in increasing urea permeability across the mucosa has been determined (Tombola et al., 2001), however whether or not it plays a role during the early stages of infection is less clear. Under acidic conditions VacA becomes active and functions in apoptosis and urea diffusion (Tombola et al., 2001). To assess this question and the potential role played by VacA in infection outcome, we simulate total extracellular levels of acid-activated VacA in the antrum and corpus (see Eqs. (A.21) and (A.22)). Lacking experimental evidence to suggest otherwise, we simulate constitutive expression of VacA in vivo at low levels and that this expression occurs at a constant rate. Under acidic conditions (pH below 2), secreted VacA is activated (Eqs. (A.22)–(A.25)) and functions as a permease (in nanomolar quantities) and a vacuolating agent (Szabo et al., 1999). We use the estimated half-life of VacA to determine the loss rate of VacA from the system using formula A.20 where κ represents the loss rate,

$$\kappa = \ln 2 / \text{Half-life}, \quad (A.20)$$

$$\frac{d[Vc(t)]_A}{dt} = \varepsilon_1([pHA_{AL}(t)])HpM_A(t) + \varepsilon_2([pHA_{AE}(t)]) \times HpA_A(t) - \rho_{VacA}[Vc(t)]_A, \quad (A.21)$$

$$\frac{d[Vc(t)]_C}{dt} = \varepsilon_3([pHA_{CL}(t)])HpM_C(t) + \varepsilon_4([pHA_{AE}(t)]) \times HpA_C(t) - \rho_{VacA}[Vc(t)]_C, \quad (A.22)$$

where

$$\varepsilon_1([pHA_{AL}(t)]) = \varepsilon_{\max} \cdot HpA_{AL}(t)(1 - (\tanh([pHA_{AL}(t)] - [A_{vcrit}]))^2), \quad (A.23)$$

$$\varepsilon_2([pHA_{AE}(t)]) = \varepsilon_{\max} \cdot HpA_{AE}(t)(1 - (\tanh([pHA_{AE}(t)] - [A_{vcrit}]))^2), \quad (A.24)$$

$$\varepsilon_3([pHA_{CL}(t)]) = \varepsilon_{\max} \cdot HpA_{CL}(t)(1 - (\tanh([pHA_{CL}(t)] - [A_{vcrit}]))^2), \quad (A.25)$$

$$\varepsilon_4([pHA_{CE}(t)]) = \varepsilon_{\max} \cdot HpA_{CE}(t)(1 - (\tanh([pHA_{CE}(t)] - [A_{vcrit}]))^2). \quad (A.26)$$

Cag protein equations. We express Cag protein dynamics in terms of production and loss (Eqs. (A.27)–(A.28)) and assume that proximity of adherent bacteria to host cells ensures that these bacteria are able to insert Cag-related effectors directly into host cells. Also, because Cag protein kinetics have not been studied, we propose that production of Cag protein is directly proportional to the number of adherent bacteria in the corpus and antrum thereby suggesting that each adherent bacterium expresses a type IV secretion apparatus. These assumptions are reasonable since type IV secretion apparatus require proximity to host epithelial cells to function (Eaton et al., 2001). We use the estimated half-life of Cag protein to define the rate of loss of Cag protein. Therefore, a balance between production and loss of Cag protein must be maintained to establish relatively constant levels of Cag proteins. To achieve this equilibrium or steady state we assume constitutive Cag protein expression. The following define the total levels of Cag protein in the antrum and corpus:

$$\frac{d[Cg(t)]_A}{dt} = \chi \cdot HpA_A(t) - \rho_{Cag}[Cg(t)]_A, \quad (A.27)$$

$$\frac{d[Cg(t)]_C}{dt} = \chi \cdot HpA_C(t) - \rho_{Cag}[Cg(t)]_C. \quad (A.28)$$

A.2. Parameter estimation for *H. pylori* Model

We outline the parameters used in our *H. pylori* Model in Table 1. These parameters include reaction, transport, decay, growth and loss rates all of which are standardized using appropriate units of measurement to allow us to perform our simulations. For estimates of all parameter values, we rely on values reported in literature and convert these values to estimates suitable for use in our model. In the cases where an appropriate parameter cannot be obtained from literature, we use mathematical estimates obtained through LHS for simulations. Mathematical estimates are also included and highlighted in Tables 1 and 2. Below we outline how we estimated parameter values.

Bacterial parameters. We consider the total bacterial population in specific regions of interest (near the lumen and epithelia in the antrum and corpus). The growth rate of *H. pylori* varies with estimates ranging from doubling times of 50 min (Andersen et al., 1997) to 11.5 h (Mendz and Hazell, 1995) depending on experimental growth conditions. For estimates of in vivo growth rates, we assume that the stomach is the optimal environment for *H. pylori* growth and thus we choose a value closer to 50 min. For bacterial loss rates, we assume that bacteria are lost at rates equivalent to epithelial sloughing for adherent bacteria (0.0139 h^{-1} ; Kirschner and Blaser, 1995) or mucus shedding for motile bacteria ($0.5\text{--}0.33 \text{ h}^{-1}$; Hattori and Arizono, 1988). There is an approximate 600% increase in host apoptosis (Szabo and Tarnawski, 2000), thus we assume it increases bacterial loss during infection as well.

The kinetics associated with ammonia production by urea hydrolysis have been well documented for *H. pylori* (Dunn et al., 1990; Scott et al., 1998). We obtained order of magnitude estimates from (Dunn et al., 1990; Scott et al., 1998). We converted mmol/l values of ammonia levels to our standard M/h units and for rates of reaction we use per hour units. Urease hydrolysis is efficient and this is reflected in literature values of the maximal rate of urea degradation ($1100 \pm 200 \text{ mM/min/mg}$; Dunn et al., 1990). Given urea degradation rate, we assume an equivalent rate of ammonia production. For clearance of ammonia from the stomach, we rely on our uncertainty analyses.

Bacteria express VacA and Cag proteins at rates that are difficult to define experimentally. Therefore, we estimate these using uncertainty analyses. Degradation rates of both these proteins are also lacking; however, these proteins are believed to be long-lived (T. Cover, personal communication). Our sensitivity analyses show that during early stages of infection variation of parameters associated with these proteins does not have a strong influence on outcome.

A.3. Host factor dynamics

Urea equations. Urea dynamics in our model are defined by a balance between availability from an extragastric source and loss due to bacterial consumption and transport out of the stomach (Eqs. (A.28)–(A.31)). Urea, a by-product of protein digestion, diffuses into the stomach from underlying blood vessel in the gastric mucosa maintaining millimolar levels of urea in the stomach (Mokuolu et al., 1997; Tombola et al., 2001). To include this, we assume that there is a constant source of urea ($\Phi = 2.77 \text{ mM}$ in the whole stomach). From our uncertainty analyses, we predict that variations within the millimolar range can be achieved without adverse effects. Therefore, we use values of 5.6 and 3.6 mM in the corpus and antrum, respectively. The

difference between corpus and antral urea source levels reflects the difference in surface areas of the two compartments (i.e. the corpus has a larger surface area than the antrum). Urea availability may also be enhanced by VacA activity in a dose-dependent manner (Tombola et al., 2001). Their results show that VacA functions as a urea permease in nanomolar quantities with a Michaelis constant of about 20 nM. During simulations, we use Michaelis–Menten kinetics to approximate the dose-dependent nature of VacA activity for mathematical simplicity (Eqs. (A.32) and (A.33)). A gradient is established from the boundaries near the epithelial surfaces to that near the lumen with higher urea levels near epithelial cells. Loss of urea occurs when both adherent and motile bacteria consume urea via Michaelis–Menten kinetics described earlier. Further loss from a given region occurs either by diffusion or transport to other regions

$$\begin{aligned} \frac{d[Ur(t)]_{AL}}{dt} = & \psi_1([pHA_{AL}(t)]) \left(\frac{[Ur(t)]_{AL}}{[Ur(t)]_{AL} + k_{UrNh}} \right) \\ & \times HpM_A(t) + diff_{UR}[Ur(t)]_{AE} \\ & - \kappa_p[Ur(t)]_{AL} + \beta_p[Ur(t)]_{CL}, \end{aligned} \quad (\text{A.29})$$

$$\begin{aligned} \frac{d[Ur(t)]_{AE}}{dt} = & \Phi_1 + i_1([Vc(t)]_A) - \psi_2([pHA_{AE}(t)]) \\ & \times \left(\frac{[Ur(t)]_{AE}}{[Ur(t)]_{AE} + k_{UrNh}} \right) HpA_A(t) \\ & - \kappa_p[Ur(t)]_{AE} + \beta_p[Ur(t)]_{CE} \\ & - diff_{UR}[Ur(t)]_{AE}, \end{aligned} \quad (\text{A.30})$$

$$\begin{aligned} \frac{d[Ur(t)]_{CL}}{dt} = & diff_{UR}[Ur(t)]_{CE} - \psi_3([pHA_{CL}(t)]) \\ & \times \left(\frac{[Ur(t)]_{CL}}{[Ur(t)]_{CL} + k_{UrNh}} \right) HpM_C(t), \\ & - \beta_p[Ur(t)]_{CL} + diff_{UR}[Ur(t)]_{CE}, \end{aligned} \quad (\text{A.31})$$

$$\begin{aligned} \frac{d[Ur(t)]_{CE}}{dt} = & \Phi_2 + i_2([Vc(t)]) - \psi_4([pHA_{CE}(t)]) \\ & \times \left(\frac{[Ur(t)]_{CE}}{[Ur(t)]_{CE} + k_{UrNh}} \right) HpA_C(t) \\ & - \beta_p[Ur(t)]_{CE}, \end{aligned} \quad (\text{A.32})$$

where

$$i_1([Vc(t)]_A) = i_{\max} \left(\frac{[Vc(t)]_A}{[Vc(t)]_A + k_{VcUr}} \right), \quad (\text{A.33})$$

$$i_2([Vc(t)]_C) = i_{\max} \left(\frac{[Vc(t)]_C}{[Vc(t)]_C + k_{VcUr}} \right). \quad (\text{A.34})$$

Host nutrient equations. For sustained survival and continued growth, *H. pylori* requires nutrients derived from its host. Nutrients consumed by *H. pylori* are complex and diverse including simple sugars, amino acids, and ions (Mendz and Hazell, 1995; Nakazawa, 2002). To simplify this, we track a ‘generic’ nutrient. We

assume that the majority of these nutrients are derived from cells undergoing natural cell death or bacterial-induced apoptosis via action of VacA and Cag proteins. Although, food may be rich in nutrients, we assume that these nutrients are too complex requiring further processing before consumption by *H. pylori*. Bacteria consumption of nutrients is governed by Monod kinetics with bacterial growth saturating at high nutrient levels. We account for the yield increase in bacterial population from food consumption by multiplying the Monod term ($[Nut(t)]/([Nut(t)] + k_N)$) by y ($y = 1 \times 10^{-15}$ M per bacteria) estimated mathematically. In addition, we assume that excess nutrients that are not consumed by bacteria are lost from the antrum and corpus at rates directly proportional to nutrient levels during mucus shedding

$$\begin{aligned} \frac{d[Nut(t)]_{AL}}{dt} &= diff_{Nut}[Nut(t)]_{AE} - \alpha_1 \cdot y([pHA_{AL}(t)]) \\ &\times \left(\frac{[Nut(t)]_{AL}}{[Nut(t)]_{AL} + k_N} \right) HpM_A(t) - \kappa_A[Nut(t)]_{AL} \\ &+ \beta_A[Nut(t)]_{CL}, \end{aligned} \quad (A.35)$$

$$\begin{aligned} \frac{d[Nut(t)]_{AE}}{dt} &= \Phi + \zeta_1([Vc(t)]_A, [Cg(t)]_A) - \alpha_2 \cdot y \cdot ([pHA_{AE}(t)]) \\ &\times \left(\frac{[Nut(t)]_{AE}}{[Nut(t)]_{AE} + k_N} \right) HpA_A(t) - \kappa_p[Nut(t)]_A \\ &+ \beta_p[Nut(t)]_C - diff_{Nut}[Nut(t)]_{AE}, \end{aligned} \quad (A.36)$$

$$\begin{aligned} \frac{d[Nut(t)]_{CL}}{dt} &= diff_{Nut}[Nut(t)]_{CE} - \alpha_3 \cdot y([pHA_{CL}(t)]) \\ &\times \left(\frac{[Nut(t)]_{CL}}{[Nut(t)]_{CL} + k_N} \right) HpM_C(t) \\ &- \beta_p[Nut(t)]_C, \end{aligned} \quad (A.37)$$

$$\begin{aligned} \frac{d[Nut(t)]_{CE}}{dt} &= \Phi + \zeta_2([Vc(t)]_C, [Cg(t)]) - \alpha_4 \cdot y([pHA_{CE}(t)]) \\ &\times \left(\frac{[Nut(t)]_{CE}}{[Nut(t)]_{CE} + k_N} \right) HpA_C(t) \\ &- \beta_p[Nut(t)]_C - diff_{Nut}[Nut(t)]_{AC}, \end{aligned} \quad (A.38)$$

where

$$\begin{aligned} \zeta_1([Vc(t)]_A, [Cg(t)]_A) &= \zeta_{\max} \left(\frac{[Vc(t)]_A}{[Vc(t)]_A + k_{VNu}} \right) \\ &+ \left(\frac{[Cg(t)]_A}{[Cg(t)]_A + k_{CNu}} \right), \end{aligned} \quad (A.39)$$

$$\begin{aligned} \zeta_2([Vc(t)]_C, [Cg(t)]_C) &= \zeta_{\max} \left(\frac{[Vc(t)]_C}{[Vc(t)]_C + k_{VNu}} \right) \\ &+ \left(\frac{[Cg(t)]_C}{[Cg(t)]_C + k_{CNu}} \right). \end{aligned} \quad (A.40)$$

A.4. Gastric acid secretion and its regulation

Previously, we defined a system of ordinary differential equations (ODE) describing gastric acid secretion and its regulation by gastric effectors. This system is comprehensive in that we account for acid secretion and its regulation and also monitor changes to cells responsible for this complex physiology. Below we outline the differential equations describing the gastric acid secretion model. For a full explanation of all terms see (Joseph et al., 2003). All parameters are defined in Tables 1 and 2.

Antral stem cells:

$$\begin{aligned} \frac{dA_{sc}(t)}{dt} &= (\gamma_{Asc})(A_{sc}(t))(C_{Asc} - A_{sc}(t)) \\ &- (p_G(t) + p_{D_A}(t))(\eta_{Asc})(A_{sc}(t)). \end{aligned} \quad (A.41)$$

Table 2
List of the parameters included in our gastric acid secretion model (Joseph et al., 2003)

Parameter	Description	Values	References	Unit
K_{NG1}	Maximal secretion rate of gastrin due to ENS stimulation per cell	6.28×10^{-17}	(Holst et al., 1987) (Nishi et al., 1985) (Campos et al., 1990)	M/h/cell
K_{NG2}	Maximal secretion rate of gastrin due to CNS stimulation per cell	8.75×10^{-17}	(Matsuno et al., 1997)	M/h/cell
K_{FG}	Maximal secretion rate of gastrin due to ENS stimulation per cell	9.39×10^{-18}	LHS	M/h/cell
α_{NG1}	Level of ENS stimulant at which rate of gastrin secretion is 50%	1.0×10^{-10}	(Holst et al., 1987)	M
α_{NG2}	Intensity of the regulator at which rate of gastrin secretion is 50%	1.0×10^{-10}	(Holst et al., 1987)	M
k_{SG}	Dissociation constant of somatostatin from gastrin receptors	9.0×10^{-11}	(Rocheville et al., 2000)	M
κ_G	Clearance rate of gastrin	11.88	(Hansen et al., 1996)	hr ⁻¹
β_G	Transport rate of gastrin from antrum to Corpus region	1.5	§	hr ⁻¹
K_{AS}	Maximal rate of secretion of	8.04×10^{-15}	§	M/h/cell

Table 2 (continued)

Parameter	Description	Values	References	Unit
K_{GS}	somatostatin due to stimulation with antrum acid Maximal rate of secretion of corpal somatostatin due to stimulation with antral gastrin	2.54×10^{-18}	(Schubert et al., 1987)	M/h/cell
α_{AS}	Acid concentration at which somatostatin secretion rate is half maximal	0.05	(Makhlouf and Schubert, 1990)	M
α_{GS}	Gastrin concentration at which somatostatin secretion rate is half maximal	5.20×10^{-12}	(Schubert et al., 1987)	M
k_{NS}	Dissociation constant of GRP from receptors on D cells	1.0×10^{-9}	(Schaffer et al., 1997)	M
κ_S	Clearance rate of somatostatin	13.86	§	hr ⁻¹
K_{NS1}	Maximal rate of secretion of antral somatostatin due enteric nervous stimulus	1.14×10^{-15}	(Schaffer et al., 1997) (Holst et al., 1987)	M/h/cell
K_{NS2}	Maximal rate of secretion of corpal somatostatin due enteric nervous stimulus	1.54×10^{-17}	(Schaffer et al., 1997)	M/h/cell
α_{NS1}	ENS levels at which antral somatostatin secretion rate is half maximal	6.28×10^{-7}	§	M
α_{NS2}	ENS levels at which corpal somatostatin secretion rate is half maximal	8.98×10^{-11}	§	M
k_{SS}	Dissociation constant of somatostatin from receptors on D cells	9.0×10^{-11}	(Rocheville et al., 2000)	M
K_{NH}	Maximal rate of histamine secretion due ENS stimulation	7.59×10^{-16}	(Pisegna et al., 2000)	M/h/cell
K_{GH}	Maximal rate of histamine secretion stimulated by gastrin transported to corpus	7.77×10^{-16}	(Andersson et al., 1999)	M/h/cell
α_{NH}	Intensity of regulator at which histamine secretion rate is half maximal	3.25×10^{-8}	(Pisegna et al., 2000)	M
α_{GH}	Gastrin levels at which histamine secretion rate is half maximal	3.0×10^{-10}	(Mardh et al., 1985) (Roche et al., 1991b) (Prinz et al., 1994) (Lawton et al., 1995) (Andersson et al., 1999) (Lindstrom and Hakanson, 2001)	M
k_{SH}	Dissociation constant of somatostatin from receptors on ECL cells	9.0×10^{-10}	(Rocheville et al., 2000)	M
κ_H	Clearance rate of histamine	11.89	(Belic et al., 1999)	hr ⁻¹
K_{NA}	Maximal rate of acid secretion due to nervous stimulation mediated through acetylcholine	2.33×10^{-11}	(Cantor et al., 1990)	M/h/cell
K_{GA}	Maximal acid secretion rate due to gastrin mediated stimulation	4.98×10^{-11}	(Kleveland et al., 1987)	M/h/cell
K_{HA}	Maximal acid secretion rate due to histamine mediated stimulation	7.96×10^{-10}	(Kleveland et al., 1987) (Norberg et al., 1986)	M/h/cell
α_{NA}	CNS levels at which acid output rate is half maximal	5.0×10^{-6}	(Mardh et al., 1985; Norberg et al., 1986)	M
α_{GA}	Gastrin levels at which acid output rate is half maximal	1.8×10^{-10}	(Roche et al., 1991a,c)	M
α_{HA}	Histamine levels at which acid output rate is half maximal	2.0×10^{-8}	(Mardh et al., 1985) (Norberg et al., 1986)	M
k_{SA}	Dissociation constant of somatostatin from receptors on parietal cells	9.0×10^{-10}	(Rocheville et al., 2000)	M

Table 2 (continued)

Parameter	Description	Values	References	Unit
β_A	Transfer rate of acid from the corpus to antrum	2.72	§	hr ⁻¹
κ_A	Wash out rate of acid	2.72	(Kreiss et al., 1998) (Van Duijn et al., 1989)	hr ⁻¹

§ denotes mathematically estimated values. M—molar; h—hour.

Corpus stem cells:

$$\begin{aligned} \frac{dC_{sc}(t)}{dt} = & (\gamma_{Csc})(C_{sc}(t))(C_{Csc} - C_{sc}(t)) \\ & + \left(\frac{g_{max}[Gtn_C(t)]^2}{[Gtn_C(t)]^2 + \alpha_{csc}^2} \right) C_{sc}(t) - (p_E(t) \\ & + p_{Dc}(t) + p_P(t))(\eta_{Csc})(C_{sc}(t)). \end{aligned} \quad (A.42)$$

Antral G cells:

$$\begin{aligned} \frac{dG(t)}{dt} = & p_G(t) \cdot \eta_{Asc} \cdot A_{sc}(t) + k_{g \max} \left(1 - \frac{[A_c(t)]^2}{[A_c(t)]^2 + \alpha_{HA}^2} \right) \\ & \times G(t) - \lambda_{fd \max} \left(1 - \frac{(Fd(t))^2}{(Fd(t))^2 + \alpha_{fd}^2} \right) \\ & \times G(t) - \lambda_{Gc} \cdot G(t). \end{aligned} \quad (A.43)$$

Antral D cells:

$$\begin{aligned} \frac{dD_A(t)}{dt} = & p_{D_A}(t) \cdot \eta_{Asc} \cdot A_{sc}(t) + \left(\frac{k_{d \max}[A_C(t)]^2}{[A_C(t)]^2 + \alpha_{HA}^2} \right) \\ & \times D(t) - \lambda_{D_A} \cdot D_A(t) + \lambda_{fd \max} \\ & \times \left(1 - \frac{(Fd(t))^2}{(Fd(t))^2 + \alpha_{fd}^2} \right) D_A(t). \end{aligned} \quad (A.44)$$

Corpus D cells:

$$\frac{dD_C(t)}{dt} = p_{D_C}(t) \cdot \eta_{Asc} \cdot C_{sc}(t) - \lambda_{D_C} \cdot D_C(t). \quad (A.45)$$

Corpus ECL cells:

$$\begin{aligned} \frac{dE(t)}{dt} = & p_E(t) \cdot \eta_{Csc} \cdot C_{sc}(t) - \lambda_E \cdot E(t) \\ & + \left(\frac{k_e \max[Gtn_c(t)]^2}{[Gtn_c(t)]^2 + \alpha_E^2} \right) E(t). \end{aligned} \quad (A.46)$$

Corpus parietal cells:

$$\frac{dP(t)}{dt} = p_P(t) \cdot \eta_{Csc} \cdot C_{sc}(t) - \lambda_P \cdot P(t). \quad (A.47)$$

A.5. Feeding function

$$\begin{aligned} Fd(t) = & 8(1 + \tanh(\pi[t - (24qrs + 19)])) \\ & \times e^{-(1/2)(1+3.5[t-(24qrs+19)])} \\ & + 5(1 + \tanh(\pi[t - (24qrs + 13)])) \\ & \times e^{-(1/2)(1+3.5[t-(24qrs+13)])} \\ & + 2(1 + \tanh(\pi[t - (24qrs + 7)])) \\ & \times e^{-(1/2)(1+3.5[t-(24qrs+7)])}, \end{aligned} \quad (A.48)$$

where

$$qrs = \text{floor}\left(\frac{t}{24}\right). \quad (A.49)$$

CNS neural effectors:

$$\begin{aligned} \frac{d[N_C(t)]}{dt} = & \left(\frac{N_{max1} Fd(t)}{(Fd(t) + k1_{fd}) \left(1 + \frac{[A_c(t)]^2}{[A_c(t)]^2 + k_{AN1}^2} \right)} \right) \\ & - \kappa_{N_C}[N_C(t)] + Bas_1. \end{aligned} \quad (A.50)$$

ENS neural effectors:

$$\begin{aligned} \frac{d[N_E(t)]}{dt} = & \left(\frac{N_{max2} Fd(t)}{(Fd(t) + k2_{fd}) \left(1 + \frac{[A_c(t)]^2}{[A_c(t)]^2 + k_{AN2}^2} \right)} \right) \\ & - \kappa_{N_E}[N_E(t)] + Bas_2. \end{aligned} \quad (A.51)$$

Antral gastrin:

$$\begin{aligned} \frac{d[Gtn_A(t)]}{dt} = & G(t) \left(\frac{K_{NG1}[N_E(t)]}{([N_E(t)] + \alpha_{NG1}) \left(1 + \frac{[S_A(t)]}{k_{SG}} \right) \left(1 + \frac{[A_c(t)]^2}{[A_c(t)]^2 + k_{AG}^2} \right)} \right. \\ & + \frac{K_{NG2}[N_C(t)]}{([N_C(t)] + a_{NG2}) \left(1 + \frac{[S_A(t)]}{k_{SG}} \right) \left(1 + \frac{[A_c(t)]^2}{[A_c(t)]^2 + k_{AG}^2} \right)} \\ & \left. + \frac{K_{FG}[Fd(t)]}{([Fd(t)] + a_{FG}) \left(1 + \frac{[S_A(t)]}{k_{SG}} \right) \left(1 + \frac{[A_c(t)]^2}{[A_c(t)]^2 + k_{AG}^2} \right)} \right) \\ & - (k_G + \beta_G)[Gtn_A(t)]. \end{aligned} \quad (A.52)$$

Corpus gastrin:

$$\frac{d[Gtn_C(t)]}{dt} = \beta_G[Gtn_A(t)] - \kappa_G[Gtn_C(t)]. \quad (\text{A.53})$$

Antral somatostatin:

$$\begin{aligned} \frac{d[S_A(t)]}{dt} &= D_A(t) \left(\left(\frac{K_{AS}[A_A(t)]}{([A_A(t)] + \alpha_{AS}) \left(1 + \frac{[S_A(t)]}{k_{SS}}\right) \left(1 + \frac{[N_C(t)]}{K_{NS}}\right)} \right) \right. \\ &\quad \left. + \left(\frac{K_{GS}[N_E(t)]}{([N_E(t)] + \alpha_{NS}) \left(1 + \frac{[S_A(t)]}{k_{SS}}\right) \left(1 + \frac{[N_C(t)]}{K_{NS}}\right)} \right) \right) \\ &\quad - \kappa_S[S_A(t)]. \end{aligned} \quad (\text{A.54})$$

Corpus somatostatin:

$$\begin{aligned} \frac{d[S_C(t)]}{dt} &= D_C(t) \left(\left(\frac{K_{NS}[N_E(t)]}{([N_E(t)] + \alpha_{NS}) \left(1 + \frac{[S_C(t)]}{k_{SS}}\right) \left(1 + \frac{[N_C(t)]}{K_{NS}}\right)} \right) \right. \\ &\quad \left. + \left(\frac{K_{GS}[Gtn_C(t)]}{([Gtn_C(t)] + \alpha_{GS}) \left(1 + \frac{[S_C(t)]}{k_{SS}}\right) \left(1 + \frac{[N_C(t)]}{K_{NS}}\right)} \right) \right) \\ &\quad - \kappa_S[S_C(t)]. \end{aligned} \quad (\text{A.55})$$

Corpus histamine:

$$\begin{aligned} \frac{d[H_C(t)]}{dt} &= E(t) \left(\left(\frac{K_{NH}[N_E(t)]}{([N_E(t)] + \alpha_{NH}) \left(1 + \frac{[S_C(t)]}{k_{SH}}\right)} \right) \right. \\ &\quad \left. + \left(\frac{K_{GH}[Gtn_C(t)]}{([Gtn_C(t)] + \alpha_{GH}) \left(1 + \frac{[S_C(t)]}{k_{SH}}\right)} \right) \right) \\ &\quad - \kappa_H[H_C(t)]. \end{aligned} \quad (\text{A.56})$$

Corpus gastric acid:

Epithelial:

$$\begin{aligned} \frac{d[A_{CE}(t)]}{dt} &= P \left(\left(\frac{K_{NA}[N_C(t)]}{([N_C(t)] + \alpha_{NA}) \left(1 + \frac{[S_C(t)]}{k_{SA}}\right)} \right) \right. \\ &\quad \left. + \left(\frac{[H_C(t)]}{[H_C(t)] + \alpha_H} \right) \right) \\ &\quad \times \left(\frac{K_{GA}[Gtn_C(t)]}{([Gtn_C(t)] + \alpha_{GA}) \left(1 + \frac{[S_C(t)]}{k_{SA}}\right)} \right) \end{aligned}$$

$$\begin{aligned} &+ \left(\frac{K_{HA}[H_C(t)]}{([H_C(t)] + \alpha_{HA}) \left(1 + \frac{[S_C(t)]}{k_{SA}}\right)} \right) \\ &\quad - hb[A_{CE}][B_{CE}] - \frac{k_f \max Fd(t)}{Fd(t) + \alpha_{FA}} [A_{CE}(t)] \\ &\quad - \sigma[NH_3(t)]_{CE} [A_{CE}(t)] - \beta[A_{CE}(t)] \\ &\quad - diff_{H^+}[A_{CE}(t)]. \end{aligned} \quad (\text{A.57})$$

Luminal:

$$\begin{aligned} \frac{d[A_{CL}(t)]}{dt} &= diff_{H^+}[A_{CE}(t)] - \beta_A[A_{CL}(t)] \\ &\quad - \sigma[NH_3(t)]_{AL} [A_{AL}(t)] \\ &\quad - hb[A_{CL}][B_{CL}]. \end{aligned} \quad (\text{A.58})$$

Antral gastric acid:

Epithelial:

$$\begin{aligned} \frac{d[A_{AE}(t)]}{dt} &= \beta_A[A_{CE}(t)] - \sigma[NH_3(t)]_{AE} [A_{AE}(t)] \\ &\quad - hb[A_{CE}][B_{CE}] - \kappa_A[A_{AE}(t)] \\ &\quad + diff_{H^+}[A_{AL}(t)]. \end{aligned} \quad (\text{A.59})$$

Luminal:

$$\begin{aligned} \frac{d[A_{AL}(t)]}{dt} &= \beta_A[A_{CL}(t)] - \sigma[NH_3(t)]_{AL} [A_{AL}(t)] \\ &\quad - hb[A_{CL}][B_{CL}] - \kappa_A[A_{AL}(t)] \\ &\quad - diff_{H^+}[A_{AL}(t)]. \end{aligned} \quad (\text{A.60})$$

Corpus bicarbonate:

$$\begin{aligned} \frac{d[B_C(t)]}{dt} &= \frac{k_{bc} \max [N_C(t)]}{[N_C(t)] + \alpha_{NB}} - hb[A_C(t)][B_C(t)] \\ &\quad - \beta_b[B_C(t)]. \end{aligned} \quad (\text{A.61})$$

Antral bicarbonate:

$$\begin{aligned} \frac{d[B_A(t)]}{dt} &= \frac{k_{bA} \max [N_C(t)]}{[N_C(t)] + \alpha_{NB}} - hb[A_A(t)][B_A(t)] \\ &\quad - \kappa_b[B_A(t)]. \end{aligned} \quad (\text{A.62})$$

References

- Achour, L., Meance, S., Briend, A., 2001. Comparison of gastric emptying of a solid and a liquid nutritional rehabilitation food. *Eur. J. Clin. Nutr.* 55 (9), 769–772.
- Andersen, A.P., Elliott, D.A., Lawson, M., Barland, P., Hatcher, V.B., Puszkun, E.G., 1997. Growth and morphological transformations of *Helicobacter pylori* in broth media. *J. Clin. Microbiol.* 35 (11), 2918–2922.
- Andersson, N., Rhedin, M., Peteri-Brunback, B., Andersson, K., Cabero, J.L., 1999. Gastrin effects on isolated rat enterochromaffin-like cells following long-term hypergastrinaemia in vivo. *Biochim. Biophys. Acta* 1451 (2–3), 297–304.
- Annibale, B., Capurso, G., Lahner, E., Passi, S., Ricci, R., Maggio, F., Delle Fave, G., 2003. Concomitant alterations in intragastric pH and ascorbic acid concentration in patients with *Helicobacter pylori* gastritis and associated iron deficiency anaemia. *Gut* 52 (4), 496–501.

- Atkinson, D.E., Bourke, E., 1987. Metabolic aspects of the regulation of systemic pH. *Am. J. Physiol.* 252 (6 Pt 2), F947–56.
- Atkinson, D.E., Camien, M.N., 1982. The role of urea synthesis in the removal of metabolic bicarbonate and the regulation of blood pH. *Curr. Top. Cell. Regul.* 21, 261–302.
- Belic, A., Grabnar, I., Karba, R., Mrhar, A., Irman-Florjanc, T., Primožic, S., 1999. Interdependence of histamine and methylhistamine kinetics: modelling and simulation approach. *Comput. Biol. Med.* 29 (6), 361–375.
- Blaser, M.J., Kirschner, D., 1999. Dynamics of *Helicobacter pylori* colonization in relation to the host response. *Proc. Natl Acad. Sci. USA* 96 (15), 8359–8364.
- Blower, S.M., Dowlatabadi, H., 1994. Sensitivity and uncertainty analysis of complex models of disease transmission: an HIV model, as an example. *Int. Stat. Rev.* 62 (2), 229–243.
- Campos, R.V., Buchan, A.M., Meloche, R.M., Pederson, R.A., Kwok, Y.N., Coy, D.H., 1990. Gastrin secretion from human antral G cells in culture. *Gastroenterology* 99 (1), 36–44.
- Cantor, P., Petersen, M.B., Christiansen, J., Rehfeld, J.F., 1990. Does sulfation of gastrin influence gastric acid secretion in man? *Scand. J. Gastroenterol.* 25 (7), 739–745.
- Cave, D.R., 2001. Chronic gastritis and *Helicobacter pylori*. *Semin. Gastrointest. Dis.* 12 (3), 196–202.
- Cave, D.R., Masubuchi, N., Goddard, P.J., 1998. Relevant factors in regulating endocrine, parietal and chief cells. In *Helicobacter pylori: Basic Mechanisms to Clinical Cure 1998: The Proceedings of a Symposium Organized by AXCAN PHARMA, San Diego, January 18–21, 1998*. Kluwer Academic Press, Dordrecht, Boston, pp. xx, 507.
- Cheema-Dhadli, S., Jungas, R.L., Halperin, M.L., 1987. Regulation of urea synthesis by acid-base balance in vivo: role of NH₃ concentration. *Am. J. Physiol.* 252 (2 Pt 2), F221–225.
- Chen, G., Fournier, R.L., Varanasi, S., Mahama-Relue, P.A., 1997. *Helicobacter pylori* survival in gastric mucosa by generation of a pH gradient. *Biophys. J.* 73 (2), 1081–1088.
- Cover, T.L., Krishna, U.S., Israel, D.A., Peek Jr., R.M., 2003. Induction of gastric epithelial cell apoptosis by *Helicobacter pylori* vacuolating cytotoxin. *Cancer Res.* 63 (5), 951–957.
- de Bernard, M., Moschioni, M., Papini, E., Telford, J., Rappuoli, R., Montecucco, C., 1998. Cell vacuolization induced by *Helicobacter pylori* VacA toxin: cell line sensitivity and quantitative estimation. *Toxicol. Lett.* 99 (2), 109–115.
- D'Elios, M.M., Manghetti, M., Almerigogna, F., Amedei, A., Costa, F., Burrioni, D., Baldari, C.T., Romagnani, S., Telford, J.L., Del Prete, G., 1997a. Different cytokine profile and antigen-specificity repertoire in *Helicobacter pylori*-specific T cell clones from the antrum of chronic gastritis patients with or without peptic ulcer. *Eur. J. Immunol.* 27 (7), 1751–1755.
- D'Elios, M.M., Manghetti, M., De Carli, M., Costa, F., Baldari, C.T., Burrioni, D., Telford, J.L., Romagnani, S., Del Prete, G., 1997b. T helper 1 effector cells specific for *Helicobacter pylori* in the gastric antrum of patients with peptic ulcer disease. *J. Immunol.* 158 (2), 962–967.
- Dunn, B.E., Campbell, G.P., Perez-Perez, G.I., Blaser, M.J., 1990. Purification and characterization of urease from *Helicobacter pylori*. *J. Biol. Chem.* 265 (16), 9464–9469.
- Eaton, K.A., 1999. Animal models of *Helicobacter gastritis*. *Curr. Top. Microbiol. Immunol.* 241, 123–154.
- Eaton, K.A., Brooks, C.L., Morgan, D.R., Krakowka, S., 1991. Essential role of urease in pathogenesis of gastritis induced by *Helicobacter pylori* in gnotobiotic piglets. *Infect. Immun.* 59 (7), 2470–2475.
- Eaton, K.A., Kersulyte, D., Mefford, M., Danon, S.J., Krakowka, S., Berg, D.E., 2001. Role of *Helicobacter pylori* cag region genes in colonization and gastritis in two animal models. *Infect. Immun.* 69 (5), 2902–2908.
- El-Omar, E.M., Carrington, M., Chow, W.H., McColl, K.E., Bream, J.H., Young, H.A., Herrera, J., Lissowska, J., Yuan, C.C., Rothman, N., Lanyon, G., Martin, M., Fraumeni Jr., J.F., Rabkin, C.S., 2000. Interleukin-1 polymorphisms associated with increased risk of gastric cancer. *Nature* 404 (6776), 398–402.
- Engel, E., Peskoff, A., Kauffman Jr., G.L., Grossman, M.I., 1984. Analysis of hydrogen ion concentration in the gastric gel mucus layer. *Am. J. Physiol.* 247 (4 Pt 1), G321–338.
- Falk, P.G., Syder, A.J., Guruge, J.L., Kirschner, D., Blaser, M.J., Gordon, J.I., 2000. Theoretical and experimental approaches for studying factors defining the *Helicobacter pylori*-host relationship. *Trends Microbiol.* 8 (7), 321–329.
- Ferrero, R.L., Lee, A., 1988. Motility of *Campylobacter jejuni* in a viscous environment: comparison with conventional rod-shaped bacteria. *J. Gen. Microbiol.* 134 (Pt 1), 53–59.
- Furuta, T., Baba, S., Takashima, M., Futami, H., Arai, H., Kajimura, M., Hanai, H., Kaneko, E., 1998. Effect of *Helicobacter pylori* infection on gastric juice pH. *Scand. J. Gastroenterol.* 33 (4), 357–363.
- Graham, D.Y., 2000. Community acquired acute *Helicobacter pylori* gastritis. *J. Gastroenterol. Hepatol.* 15 (12), 1353–1355.
- Graham, D.Y., Alpert, L.C., Smith, J.L., Yoshimura, H.H., 1988. Iatrogenic *Campylobacter pylori* infection is a cause of epidemic achlorhydria. *Am. J. Gastroenterol.* 83 (9), 974–980.
- Hansen, C.P., Stadil, F., Yucun, L., Rehfeld, J.F., 1996. Pharmacokinetics and organ metabolism of carboxamidated and glycine-extended gastrins in pigs. *Am. J. Physiol.* 271 (1 Pt 1), G156–163.
- Hattori, T., Arizono, N., 1988. Cell kinetics and secretion of mucus in the gastrointestinal mucosa, and their diurnal rhythm. *J. Clin. Gastroenterol.* 10 (Suppl. 1), S1–6.
- Hersey, S.J., Sachs, G., 1995. Gastric acid secretion. *Physiol. Rev.* 75 (1), 155–189.
- Hessey, S.J., Spencer, J., Wyatt, J.I., Sobala, G., Rathbone, B.J., Axon, A.T., Dixon, M.F., 1990. Bacterial adhesion and disease activity in *Helicobacter* associated chronic gastritis. *Gut* 31 (2), 134–138.
- Holst, J.J., Knuhtsen, S., Orskov, C., Skak-Nielsen, T., Poulsen, S.S., Nielsen, O.V., 1987. GRP-producing nerves control antral somatostatin and gastrin secretion in pigs. *Am. J. Physiol.* 253 (6 Pt 1), G767–774.
- Huesca, M., Gold, B., Sherman, P., Lewin, P., Lingwood, C., 1993. Therapeutics used to alleviate peptic ulcers inhibit *H. pylori* receptor binding in vitro. *Zentralbl. Bakteriologie* 280 (1–2), 244–252.
- Hwang, I.R., Kodama, T., Kikuchi, S., Sakai, K., Peterson, L.E., Graham, D.Y., Yamaoka, Y., 2002. Effect of interleukin 1 polymorphisms on gastric mucosal interleukin 1beta production in *Helicobacter pylori* infection. *Gastroenterology* 123 (6), 1793–1803.
- Ibraghimov, A., Pappo, J., 2000. The immune response against *Helicobacter pylori*—a direct linkage to the development of gastroduodenal disease. *Microbes. Infect.* 2 (9), 1073–1077.
- Iman, R.L., Helton, J.C., Campbell, J.E., 1981a. An approach to sensitivity analysis of computer models: Part I — Introduction, input variable selection and preliminary variable assessment. *J. Qual. Technol.* 13, 174–183.
- Iman, R.L., Helton, J.C., Campbell, J.E., 1981b. An approach to sensitivity analysis of computer models: Part II—Ranking of input variables, response surface validation, distribution effect and technique synopsis. *J. Qual. Technol.* 13, 232–240.
- Jones, N.L., Day, A.S., Jennings, H.A., Sherman, P.M., 1999. *Helicobacter pylori* induces gastric epithelial cell apoptosis in association with increased Fas receptor expression. *Infect. Immun.* 67 (8), 4237–4242.
- Josenshans, C., Suerbaum, S., 2002. The role of motility as a virulence factor in bacteria. *Int. J. Med. Microbiol.* 291 (8), 605–614.

- Joseph, I.M., Zavros, Y., Merchant, J.L., Kirschner, D., 2003. A model for integrative study of human gastric acid secretion. *J. Appl. Physiol.* 94 (4), 1602–1618.
- Kamisago, S., Iwamori, M., Tai, T., Mitamura, K., Yazaki, Y., Sugano, K., 1996. Role of sulfatides in adhesion of *Helicobacter pylori* to gastric cancer cells. *Infect. Immun.* 64 (2), 624–628.
- Kapadia, C.R., 2003. Gastric atrophy, metaplasia, and dysplasia: a clinical perspective. *J. Clin. Gastroenterol.* 36 (5), S29–36.
- Karita, M., Tsuda, M., Nakazawa, T., 1995. Essential role of urease in vitro and in vivo *Helicobacter pylori* colonization study using a wild-type and isogenic urease mutant strain. *J. Clin. Gastroenterol.* 21 (Suppl. 1), S160–163.
- Kirschner, D., 1999. Dynamics of co-infection with *M. Tuberculosis* and HIV-1. *Theor. Popul. Biol.* 55 (1), 94–109.
- Kirschner, D.E., Blaser, M.J., 1995. The dynamics of *Helicobacter pylori* infection of the human stomach. *J. Theor. Biol.* 176 (2), 281–290.
- Kitahara, F., Shimazaki, R., Sato, T., Kojima, Y., Morozumi, A., Fujino, M.A., 1998. Severe atrophic gastritis with *Helicobacter pylori* infection and gastric cancer. *Gastric Cancer* 1 (2), 118–124.
- Kleveland, P.M., Waldum, H.L., Larsson, H., 1987. Gastric acid secretion in the totally isolated, vascularly perfused rat stomach. A selective muscarinic-1 agent does, whereas gastrin does not, augment maximal histamine-stimulated acid secretion. *Scand. J. Gastroenterol.* 22 (6), 705–713.
- Konturek, P.C., Brzozowski, T., Karczewska, E., Duda, A., Bielanski, W., Hahn, E.G., Konturek, S.J., 2000. Water extracts of *Helicobacter pylori* suppress the expression of histidine decarboxylase and reduce histamine content in the rat gastric mucosa. *Digestion* 62 (2–3), 100–109.
- Kreiss, C., Schwizer, W., Borovicka, J., Jansen, J.B., Bouloux, C., Pignol, R., Bischof Delaloye, A., Fried, M., 1998. Effect of linitript, a new CCK—A receptor antagonist, on gastric emptying of a solid-liquid meal in humans. *Regul. Pept.* 74 (2–3), 143–149.
- Lawton, G.P., Tang, L.H., Miu, K., Gilligan, C.J., Absood, A., Modlin, I.M., 1995. Adrenergic and cromolyn sodium modulation of ECL cell histamine secretion. *J. Surg. Res.* 58 (1), 96–104.
- Lee, A., 1998. Animal models for host–pathogen interaction studies. *Br. Med. Bull.* 54 (1), 163–173.
- Lee, A., 1999. Animal models of *Helicobacter* infection. *Mol. Med. Today* 5 (11), 500–501.
- Lindstrom, E., Hakanson, R., 2001. Neurohormonal regulation of secretion from isolated rat stomach ECL cells: a critical reappraisal. *Regul. Pept.* 97 (2–3), 169–180.
- Mahalanabis, D., Rahman, M.M., Sarker, S.A., Bardhan, P.K., Hildebrand, P., Beglinger, C., Gyr, K., 1996. *Helicobacter pylori* infection in the young in Bangladesh: prevalence, socioeconomic and nutritional aspects. *Int. J. Epidemiol.* 25 (4), 894–898.
- Makhlouf, G.M., Schubert, M.L., 1990. Gastric somatostatin: a paracrine regulator of acid secretion. *Metabolism* 39 (9 Suppl. 2), 138–142.
- Marchetti, M., Arico, B., Burrioni, D., Figura, N., Rappuoli, R., Ghiara, P., 1995. Development of a mouse model of *Helicobacter pylori* infection that mimics human disease. *Science* 267 (5204), 1655–1658.
- Mardh, S., Norberg, L., Ljungstrom, M., Wollert, S., Nyren, O., Gustavsson, S., 1985. A method for in vitro studies on acid formation in human parietal cells. Stimulation by histamine, pentagastrin and carbachol. *Acta Physiol. Scand.* 123 (3), 349–354.
- Matsuno, M., Matsui, T., Iwasaki, A., Arakawa, Y., 1997. Role of acetylcholine and gastrin-releasing peptide (GRP) in gastrin secretion. *J. Gastroenterol.* 32 (5), 579–586.
- McGowan, C.C., Cover, T.L., Blaser, M.J., 1996. *Helicobacter pylori* and gastric acid: biological and therapeutic implications. *Gastroenterology* 110 (3), 926–938.
- Megraud, F., 2001. Impact of *Helicobacter pylori* virulence on the outcome of gastroduodenal diseases: lessons from the microbiologist. *Dig. Dis.* 19 (2), 99–103.
- Mendz, G.L., Hazell, S.L., 1995. Amino acid utilization by *Helicobacter pylori*. *Int. J. Biochem. Cell. Biol.* 27 (10), 1085–1093.
- Moayyedi, P., Wason, C., Peacock, R., Walan, A., Bardhan, K., Axon, A.T., Dixon, M.F., 2000. Changing patterns of *Helicobacter pylori* gastritis in long-standing acid suppression. *Helicobacter* 5 (4), 206–214.
- Mokuolu, A.O., Sigal, S.H., Lieber, C.S., 1997. Gastric juice urease activity as a diagnostic test for *Helicobacter pylori* infection. *Am. J. Gastroenterol.* 92 (4), 644–648.
- Mollenhauer-Rektorschek, M., Hanauer, G., Sachs, G., Melchers, K., 2002. Expression of UreI is required for intragastric transit and colonization of gerbil gastric mucosa by *Helicobacter pylori*. *Res. Microbiol.* 153 (10), 659–666.
- Montecucco, C., Papini, E., de Bernard, M., Zoratti, M., 1999. Molecular and cellular activities of *Helicobacter pylori* pathogenic factors. *FEBS Lett.* 452 (1–2), 16–21.
- Morris, A., Nicholson, G., 1987. Ingestion of *Campylobacter pyloridis* causes gastritis and raised fasting gastric pH. *Am. J. Gastroenterol.* 82 (3), 192–199.
- Mullins, P.D., Steer, H.W., 1998. *Helicobacter pylori* colonization density and gastric acid output in non-ulcer dyspepsia and duodenal ulcer disease. *Helicobacter* 3 (2), 86–92.
- Nagata, K., Nagata, Y., Sato, T., Fujino, M.A., Nakajima, K., Tamura, T., 2003. L-Serine, D- and L-proline and alanine as respiratory substrates of *Helicobacter pylori*: correlation between in vitro and in vivo amino acid levels. *Microbiology* 149 (Pt 8), 2023–2030.
- Nakazawa, T., 2002. Growth cycle of *Helicobacter pylori* in gastric mucous layer. *Keio J. Med.* 51 (Suppl. 2), 15–19.
- Nedrud, J.G., 1999. Animal models for gastric *Helicobacter* immunology and vaccine studies. *FEMS Immunol. Med. Microbiol.* 24 (2), 243–250.
- Nishi, S., Seino, Y., Takemura, J., Ishida, H., Seno, M., Chiba, T., Yanaihara, C., Yanaihara, N., Imura, H., 1985. Vagal regulation of GRP, gastric somatostatin, and gastrin secretion in vitro. *Am. J. Physiol.* 248 (4 Pt 1), E425–431.
- Norberg, L., Ljungstrom, M., Vega, F.V., Mardh, S., 1986. Stimulation of acid formation by histamine, carbachol and pentagastrin in isolated pig parietal cells. *Acta Physiol. Scand.* 126 (3), 385–390.
- Odenbreit, S., Puls, J., Sedlmaier, B., Gerland, E., Fischer, W., Haas, R., 2000. Translocation of *Helicobacter pylori* CagA into gastric epithelial cells by type IV secretion. *Science* 287 (5457), 1497–1500.
- Ogura, K., Maeda, S., Nakao, M., Watanabe, T., Tada, M., Kyutoku, T., Yoshida, H., Shiratori, Y., Omata, M., 2000. Virulence factors of *Helicobacter pylori* responsible for gastric diseases in Mongolian gerbil. *J. Exp. Med.* 192 (11), 1601–1610.
- Ohara, T., Goshi, S., Taneike, I., Tamura, Y., Zhang, H.M., Yamamoto, T., 2001. Inhibitory action of a novel proton pump inhibitor, rabeprazole, and its thioether derivative against the growth and motility of clarithromycin-resistant *Helicobacter pylori*. *Helicobacter* 6 (2), 125–129.
- Papini, E., Satin, B., Norais, N., de Bernard, M., Telford, J.L., Rappuoli, R., Montecucco, C., 1998. Selective increase of the permeability of polarized epithelial cell monolayers by *Helicobacter pylori* vacuolating toxin. *J. Clin. Invest.* 102 (4), 813–820.
- Park, S.M., Park, H.S., 1993. G- and D-cell populations, serum and tissue concentrations of gastrin and somatostatin in patients with peptic ulcer diseases. *Korean J. Intern. Med.* 8 (1), 1–7.
- Park, S.M., Lee, H.R., Kim, J.G., Park, J.W., Jung, G., Han, S.H., Cho, J.H., Kim, M.K., 1999. Effect of *Helicobacter pylori* infection on antral gastrin and somatostatin cells and on serum gastrin concentrations. *Korean J. Intern. Med.* 14 (1), 15–20.

- Pelicic, V., Reyrat, J.M., Sartori, L., Pagliaccia, C., Rappuoli, R., Telford, J.L., Montecucco, C., Papini, E., 1999. *Helicobacter pylori* VacA cytotoxin associated with the bacteria increases epithelial permeability independently of its vacuolating activity. *Microbiology* 145 (Pt 8), 2043–2050.
- Pisegna, J.R., Ohning, G.V., Athmann, C., Zeng, N., Walsh, J.H., Sachs, G., 2000. Role of PACAP1 receptor in regulation of ECL cells and gastric acid secretion by pituitary adenylate cyclase activating peptide. *Ann. N. Y. Acad. Sci.* 921, 233–241.
- Prinz, C., Hafsi, N., Voland, P., 2003. *Helicobacter pylori* virulence factors and the host immune response: implications for therapeutic vaccination. *Trends Microbiol.* 11 (3), 134–138.
- Prinz, C., Scott, D.R., Hurwitz, D., Helander, H.F., Sachs, G., 1994. Gastrin effects on isolated rat enterochromaffin-like cells in primary culture. *Am. J. Physiol.* 267 (4 Pt 1), G663–675.
- Queiroz, D.M., Mendes, E.N., Rocha, G.A., Cunha-Melo, J.R., Barbosa, A.J., Lima Jr., G.F., Oliveira, C.A., 1991. *Helicobacter pylori* and gastric histamine concentrations. *J. Clin. Pathol.* 44 (7), 612–613.
- Queiroz, D.M., Mendes, E.N., Rocha, G.A., Moura, S.B., Resende, L.M., Cunha-Melo, J.R., Coelho, L.G., Passos, M.C., Oliveira, C.A., Lima Junior, G.F. et al., 1993. Histamine content of the oxyntic mucosa from duodenal ulcer patients: effect of *Helicobacter pylori* eradication. *Am. J. Gastroenterol.* 88 (8), 1228–1232.
- Rad, R., Prinz, C., Neu, B., Neuhofer, M., Zeitner, M., Voland, P., Becker, I., Schepp, W., Gerhard, M., 2003. Synergistic effect of *Helicobacter pylori* virulence factors and interleukin-1 polymorphisms for the development of severe histological changes in the gastric mucosa. *J. Infect. Dis.* 188 (2), 272–281.
- Ramsey, E.J., Carey, K.V., Peterson, W.L., Jackson, J.J., Murphy, F.K., Read, N.W., Taylor, K.B., Trier, J.S., Fordtran, J.S., 1979. Epidemic gastritis with hypochlorhydria. *Gastroenterology* 76 (6), 1449–1457.
- Rektorschek, M., Buhmann, A., Weeks, D., Schwan, D., Bensch, K.W., Eskandari, S., Scott, D., Sachs, G., Melchers, K., 2000. Acid resistance of *Helicobacter pylori* depends on the UreI membrane protein and an inner membrane proton barrier. *Mol. Microbiol.* 36 (1), 141–152.
- Roche, S., Gusdinari, T., Bali, J.P., Magous, R., 1991a. Biphasic kinetics of inositol 1,4,5-trisphosphate accumulation in gastrin-stimulated parietal cells. Effects of pertussis toxin and extracellular calcium. *FEBS Lett.* 282 (1), 147–151.
- Roche, S., Gusdinari, T., Bali, J.P., Magous, R., 1991b. “Gastrin” and “CCK” receptors on histamine- and somatostatin-containing cells from rabbit fundic mucosa-II. Characterization by means of selective antagonists (L-364,718 and L-365,260). *Biochem. Pharmacol.* 42 (4), 771–776.
- Roche, S., Gusdinari, T., Bali, J.P., Magous, R., 1991c. Relationship between inositol 1,4,5- trisphosphate mass level and [14C]aminopyrine uptake in gastrin-stimulated parietal cells. *Mol. Cell. Endocrinol.* 77 (1–3), 109–113.
- Rocheville, M., Lange, D.C., Kumar, U., Sasi, R., Patel, R.C., Patel, Y.C., 2000. Subtypes of the somatostatin receptor assemble as functional homo- and heterodimers. *J. Biol. Chem.* 275 (11), 7862–7869.
- Rosberg, K., Berglindh, T., Gustavsson, S., Hubinette, R., Rolfsen, W., 1991. Adhesion of *Helicobacter pylori* to human gastric mucosal biopsy specimens cultivated in vitro. *Scand. J. Gastroenterol.* 26 (11), 1179–1187.
- Sachs, G., Scott, D., Weeks, D., Melchers, K., 2000. Gastric habitation by *Helicobacter pylori*: insights into acid adaptation. *Trends Pharmacol. Sci.* 21 (11), 413–416.
- Sachs, G., Weeks, D.L., Melchers, K., Scott, D.R., 2003. The gastric biology of *Helicobacter pylori*. *Annu. Rev. Physiol.* 65, 349–369.
- Sanduleanu, S., Jonkers, D., de Bruine, A., Hameeteman, W., Stockbrugger, R.W., 2001. Changes in gastric mucosa and luminal environment during acid-suppressive therapy: a review in depth. *Dig. Liver. Dis.* 33 (8), 707–719.
- Schaffer, K., Herrmuth, H., Mueller, J., Coy, D.H., Wong, H.C., Walsh, J.H., Classen, M., Schusdziarra, V., Schepp, W., 1997. Bombesin-like peptides stimulate somatostatin release from rat fundic D cells in primary culture. *Am. J. Physiol.* 273(3 Pt 1), G686–695.
- Schreiber, S., Nguyen, T.H., Stuben, M., Scheid, P., 2000. Demonstration of a pH gradient in the gastric gland of the acid-secreting guinea pig mucosa. *Am. J. Physiol. Gastrointest. Liver Physiol.* 279 (3), G597–604.
- Schubert, M.L., Edwards, N.F., Arimura, A., Makhlof, G.M., 1987. Paracrine regulation of gastric acid secretion by fundic somatostatin. *Am. J. Physiol.* 252 (4 Pt 1), G485–490.
- Scott, D.R., Weeks, D., Hong, C., Postius, S., Melchers, K., Sachs, G., 1998. The role of internal urease in acid resistance of *Helicobacter pylori*. *Gastroenterology* 114 (1), 58–70.
- Scott, D.R., Marcus, E.A., Weeks, D.L., Lee, A., Melchers, K., Sachs, G., 2000. Expression of the *Helicobacter pylori* ureI gene is required for acidic pH activation of cytoplasmic urease. *Infect. Immun.* 68 (2), 470–477.
- Scott, D.R., Marcus, E.A., Weeks, D.L., Sachs, G., 2002. Mechanisms of acid resistance due to the urease system of *Helicobacter pylori*. *Gastroenterology* 123 (1), 187–195.
- Shulkes, A., Read, M., 1991. Regulation of somatostatin secretion by gastrin- and acid-dependent mechanisms. *Endocrinology* 129 (5), 2329–2334.
- Sidebotham, R.L., Worku, M.L., Karim, Q.N., Dhir, N.K., Baron, J.H., 2003. How *Helicobacter pylori* urease may affect external pH and influence growth and motility in the mucus environment: evidence from in-vitro studies. *Eur. J. Gastroenterol. Hepatol.* 15 (4), 395–401.
- Solnick, J.V., Hansen, L.M., Canfield, D.R., Parsonnet, J., 2001. Determination of the infectious dose of *Helicobacter pylori* during primary and secondary infection in rhesus monkeys (*Macaca mulatta*). *Infect. Immun.* 69 (11), 6887–6892.
- Suzuki, H., Yanaka, A., Shibahara, T., Matsui, H., Nakahara, A., Tanaka, N., Muto, H., Momoi, T., Uchiyama, Y., 2002. Ammonia-induced apoptosis is accelerated at higher pH in gastric surface mucous cells. *Am. J. Physiol. Gastrointest. Liver Physiol.* 283 (4), G986–995.
- Szabo, I., Tarnawski, A.S., 2000. Apoptosis in the gastric mucosa: molecular mechanisms, basic and clinical implications. *J. Physiol. Pharmacol.* 51 (1), 3–15.
- Szabo, I., Brutsche, S., Tombola, F., Moschioni, M., Satin, B., Telford, J.L., Rappuoli, R., Montecucco, C., Papini, E., Zoratti, M., 1999. Formation of anion-selective channels in the cell plasma membrane by the toxin VacA of *Helicobacter pylori* is required for its biological activity. *EMBO. J.* 18 (20), 5517–5527.
- Takimoto, T., Satoh, K., Taniguchi, Y., Saifuku, K., Kihira, K., Seki, M., Yoshida, Y., Ido, K., Kimura, K., 1997. The efficacy and safety of one-week triple therapy with lansoprazole, clarithromycin, and metronidazole for the treatment of *Helicobacter pylori* infection in Japanese patients. *Helicobacter* 2 (2), 86–91.
- Thomsen, L.L., Gavin, J.B., Tasman-Jones, C., 1990. Relation of *Helicobacter pylori* to the human gastric mucosa in chronic gastritis of the antrum. *Gut* 31 (11), 1230–1236.
- Tombola, F., Oregna, F., Brutsche, S., Szabo, I., Del Giudice, G., Rappuoli, R., Montecucco, C., Papini, E., Zoratti, M., 1999. Inhibition of the vacuolating and anion channel activities of the VacA toxin of *Helicobacter pylori*. *FEBS Lett.* 460 (2), 221–225.
- Tombola, F., Morbiato, L., Del Giudice, G., Rappuoli, R., Zoratti, M., Papini, E., 2001. The *Helicobacter pylori* VacA toxin is a urea permease that promotes urea diffusion across epithelia. *J. Clin. Invest.* 108 (6), 929–937.

- Tsuda, M., Karita, M., Mizote, T., Morshed, M.G., Okita, K., Nakazawa, T., 1994a. Essential role of *Helicobacter pylori* urease in gastric colonization: definite proof using a urease-negative mutant constructed by gene replacement. *Eur. J. Gastroenterol. Hepatol.* 6 (Suppl. 1), S49–52.
- Tsuda, M., Karita, M., Morshed, M.G., Okita, K., Nakazawa, T., 1994b. A urease-negative mutant of *Helicobacter pylori* constructed by allelic exchange mutagenesis lacks the ability to colonize the nude mouse stomach. *Infect. Immun.* 62 (8), 3586–3589.
- Tsutsui, N., Taneike, I., Ohara, T., Goshi, S., Kojio, S., Iwakura, N., Matsumaru, H., Wakisaka-Saito, N., Zhang, H.M., Yamamoto, T., 2000. A novel action of the proton pump inhibitor rabeprazole and its thioether derivative against the motility of *Helicobacter pylori*. *Antimicrob. Agents Chemother.* 44 (11), 3069–3073.
- Uemura, N., Okamoto, S., Yamamoto, S., Matsumura, N., Yamaguchi, S., Yamakido, M., Taniyama, K., Sasaki, N., Schlemper, R.J., 2001. *Helicobacter pylori* infection and the development of gastric cancer. *N. Engl. J. Med.* 345 (11), 784–789.
- Ulmer, H.J., Beckerling, A., Gatz, G., 2003. Recent use of proton pump inhibitor-based triple therapies for the eradication of *H. pylori*: a broad data review. *Helicobacter* 8 (2), 95–104.
- Uvnas-Wallensten, K., Efendic, S., Johansson, C., Sjodin, L., Cranwell, P.D., 1980. Effect of intraluminal pH on the release of somatostatin and gastrin into antral, bulbar and ileal pouches of conscious dogs. *Acta Physiol. Scand.* 110 (4), 391–400.
- Van Duijn, B., Ypey, D.L., de Goede, J., Verveen, A.A., Hekkens, W., 1989. A model study of the regulation of gastric acid secretion. *Am. J. Physiol.* 257 (1 Pt 1), G157–168.
- Webb, G.F., Blaser, M.J., 2002. Dynamics of bacterial phenotype selection in a colonized host. *Proc. Natl. Acad. Sci. USA* 99 (5), 3135–3140.
- Weeks, D.L., Eskandari, S., Scott, D.R., Sachs, G., 2000. A H⁺-gated urea channel: the link between *Helicobacter pylori* urease and gastric colonization. *Science* 287 (5452), 482–485.
- Weeks, D.L., Sachs, G., 2001. Sites of pH regulation of the urea channel of *Helicobacter pylori*. *Mol. Microbiol.* 40 (6), 1249–1259.
- Whitehead, R., Truelove, S.C., Gear, M.W., 1972. The histological diagnosis of chronic gastritis in fiberoptic gastroscope biopsy specimens. *J. Clin. Pathol.* 25 (1), 1–11.
- Williams, C.L., Preston, T., Hossack, M., Slater, C., McColl, K.E., 1996. *Helicobacter pylori* utilizes urea for amino acid synthesis. *FEMS Immunol. Med. Microbiol.* 13 (1), 87–94.
- Wolfe, M.M., Nompleggi, D.J., 1992. Cytokine inhibition of gastric acid secretion—a little goes a long way. *Gastroenterology* 102 (6), 2177–2178.
- Zavros, Y., Paterson, A., Lambert, J., Shulkes, A., 2000. Expression of progastrin-derived peptides and somatostatin in fundus and antrum of nonulcer dyspepsia subjects with and without *Helicobacter pylori* infection. *Dig. Dis. Sci.* 45 (10), 2058–2064.